

AD-A171 678

INTRINSIC MECHANISMS OF MULTI-LAYER CERAMIC CAPACITOR
FAILURE(U) VIRGINIA POLYTECHNIC INST AND STATE UNIV
BLACKSBURG COLL OF ENGINEERING L C BURTON APR 86

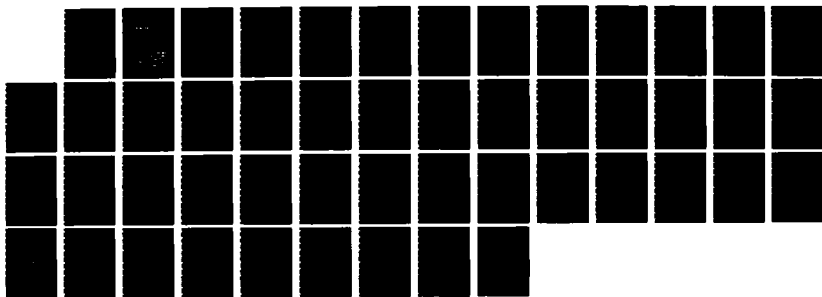
1/1

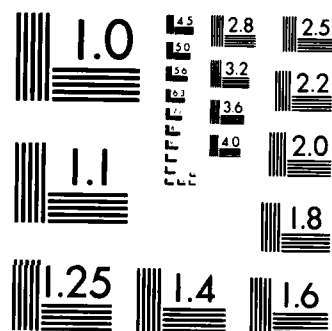
UNCLASSIFIED

N00014-83-K-0168

F/G 9/1

ML



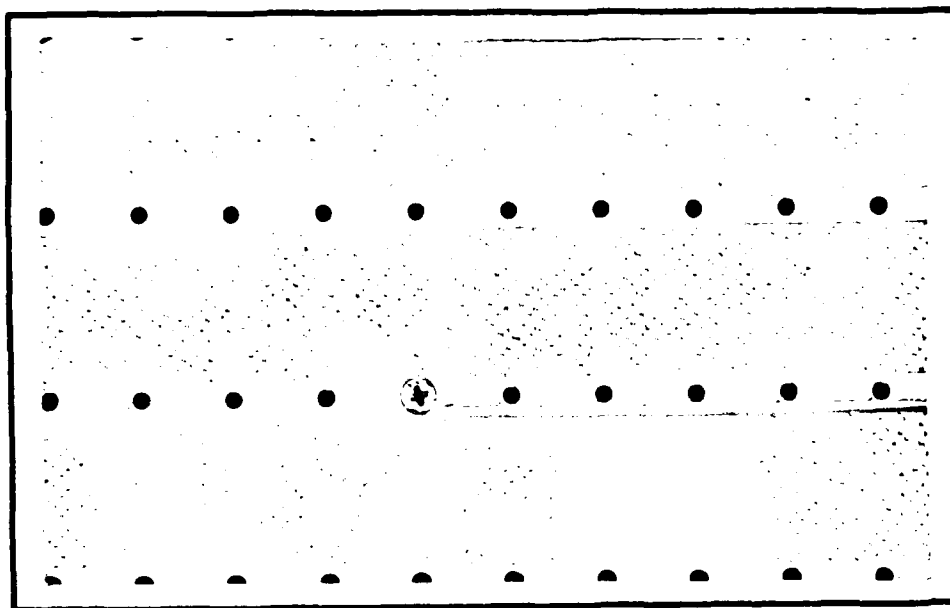


MICROCOPY RESOLUTION TEST CHART
NATIONAL BUREAU OF STANDARDS-1963-A

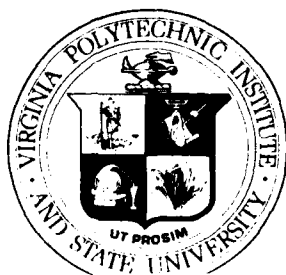
AD-A171 678

(12)

**COLLEGE
OF
ENGINEERING**



**VIRGINIA
POLYTECHNIC
INSTITUTE
AND
STATE
UNIVERSITY**



DTIC FILE COPY

**BLACKSBURG,
VIRGINIA**

12

INTRINSIC MECHANISMS OF MULTI-LAYER
CERAMIC CAPACITOR FAILURE

ANNUAL REPORT

Time Period: 3/15/85-3/14/86
ONR Contract No. N00014-83-K-0168
Principal Investigator: L. C. Burton

April 1986

Departments of Electrical Engineering and Materials Engineering
Virginia Polytechnic Institute and State University
Blacksburg, Virginia 24061

LYTIC
ELECTRONICS

SEP 4 1986

RECEIVED
SEP 4 1986

AD-A171 678

REPORT DOCUMENTATION PAGE

1a REPORT SECURITY CLASSIFICATION Unclassified			1b RESTRICTIVE MARKINGS		
2a SECURITY CLASSIFICATION AUTHORITY			3 DISTRIBUTION/AVAILABILITY OF REPORT Approved for Public Release Distribution Unlimited		
2b DECLASSIFICATION/DOWNGRADING SCHEDULE					
4 PERFORMING ORGANIZATION REPORT NUMBER(S)			5 MONITORING ORGANIZATION REPORT NUMBER(S)		
6a. NAME OF PERFORMING ORGANIZATION VPI & SU		6b. OFFICE SYMBOL (If applicable)		7a. NAME OF MONITORING ORGANIZATION	
6c. ADDRESS (City, State and ZIP Code) EE Dept. Blacksburg, VA 24061		7b. ADDRESS (City, State and ZIP Code)			
8a. NAME OF FUNDING/SPONSORING ORGANIZATION Office of Naval Research		8b. OFFICE SYMBOL (If applicable)		9 PROCUREMENT INSTRUMENT IDENTIFICATION NUMBER N00014-83-K-0168	
8c. ADDRESS (City, State and ZIP Code) Division of Materials Research Arlington, VA 22217		10 SOURCE OF FUNDING NUMS PROGRAM ELEMENT NO		PROJECT NO	TASK NO
11 TITLE (Include Security Classification) Intrinsic Mechanisms of Multilayer Ceramic Capacitor Failure					WORK UNIT NO
12. PERSONAL AUTHOR(S) L. C. Burton					
13a. TYPE OF REPORT Annual		13b. TIME COVERED FROM 3/15/85 TO 3/14/86		14 DATE OF REPORT (Yr. Mo. Day) 1986 April	
15 PAGE COUNT					
16. SUPPLEMENTARY NOTATION					
17 COSATI CODES FIELD GROUP SUB. GR.			18 SUBJECT TERMS (Continue on reverse if necessary and identify by block number) Multilayer Capacitors Leakage Currents Ferroelectric Ceramic Grain Boundaries MLC Capacitors Degradation & Reliability		
19. ABSTRACT (Continue on reverse if necessary and identify by block number) It has been established that the dominant charge carrier of leakage current in the BaTiO ₃ based X7R ceramic that we have measured is the electron. Galvanic cell measurements yield oxygen ion transport numbers of essentially zero. The major effect of oxygen movement is not ionic current, but degradation. A generic degradation current-time curve is discussed. Two models for leakage current vs time are presented: one based on oxygen vacancy (and conduction electron) increase; the other on grain boundary barrier height reduction. Both predict exponential or near-exponential increase of leakage current with time, which has been reported. Reasons for the decrease in activation energy with degradation are discussed. This is attributed to decrease in polaron hopping or grain boundary potentials, or both. The role of grain boundaries (GB) is discussed in some detail. GB impedance depends on donor density, grain boundary trap density, grain size and dielectric constant, and may or may not be significant (i.e. > 0.1eV) depending on values of these parameters. GB barrier height dependence on donor density and grain size is shown, for fixed values of the					
20 DISTRIBUTION/AVAILABILITY OF ABSTRACT UNCLASSIFIED/UNLIMITED <input type="checkbox"/> SAME AS RPT <input type="checkbox"/> DTIC USERS <input type="checkbox"/>			21 ABSTRACT SECURITY CLASSIFICATION		
22a. NAME OF RESPONSIBLE INDIVIDUAL		22b. TELEPHONE NUMBER (Include Area Code)		22c. OFFICE SYMBOL	

19. ABSTRACT (Continued)

other parameters.

Complex impedance-frequency measurements are reported for several BaTiO_3 based samples. What is possibly GB resistance is evident on X7R type ceramic; this is not evident on NPO or Z5U type ceramic. GB and contact resistance contributions are evident for $\text{Ba}_{1.01}\text{TiO}_3$, but not for $\text{Ba}_{.99}\text{TiO}_3$. The utility of voltage bias during impedance measurements is discussed, and shown to be valid for a varistor. This technique will be applied to capacitor ceramic.

Measurements were completed on a set of X7R plates polished to thicknesses from 0.22 to 2.2mm. Ohmic and super-ohmic regions are evident on all I-V curves; the latter region is attributed to space charge, and dependent on measuring ambient. Bulk and surface resistances don't depend on ambient, indicating that the SCLC ambient sensitivity is an interfacial effect. Neither resistivity nor dielectric constant depend on simple thickness.

The leakage current setup was automated, using an IBM PC-X7 computer, Keithley 705 scanner and 617 electrometer, and Okidata printer.



Accession For	
NTIS GRA&I	
DTIC TAB	
Unannounced	
Justification	
By	
Distribution	
Availability	
Dist	
A1	

TABLE OF CONTENTS

	Page
Summary of Results	1
1. Introduction	1
2. Nature of Leakage Current	2
3. Role of Grain Boundaries	14
4. Electrode-Ceramic Interface; Dielectric Thickness.	34
5. Instrumentation	38
6. Future Work	41
References	41
Appendix	43

SUMMARY OF RESULTS

It has been established that the dominant charge carrier for leakage current in the BaTiO₃ based X7R ceramic that we have measured is the electron. Galvanic cell measurements yield oxygen ion transport numbers of essentially zero. The major effect of oxygen movement is not ionic current, but degradation. A generic degradation current-time curve is discussed. Two models for leakage current vs time are presented: one based on oxygen vacancy (and conduction electron) increase; the other on grain boundary barrier height reduction. Both predict exponential or near-exponential increase of leakage current with time, which has been reported.

Reasons for the decrease in activation energy with degradation are discussed. This is attributed to decrease in polaron hopping or grain boundary potentials, or both.

The role of grain boundaries (GB) is discussed in some detail. GB impedance depends on donor density, grain boundary trap density, grain size and dielectric constant, and may or may not be significant (i.e. $> 0.1\text{eV}$) depending of values of these parameters. GB barrier height dependence on donor density and grain size is shown, for fixed values of the other parameters.

Complex impedance-frequency measurements are reported for several BaTiO₃ based samples. What is possibly GB resistance is evident on X7R type ceramic; this is not evident on NPO or Z5U type ceramic. GB and contact resistance contributions are evident for Ba_{1.01}TiO₃ but not for Ba_{0.99}TiO₃. The utility of voltage bias during impedance measurements is discussed, and shown to be valid for a varistor. This technique will be applied to capacitor ceramic.

Measurements were completed on a set of X7R plates polished to thicknesses from 0.22 to 2.2 mm. Ohmic and super-ohmic regions are evident on all I-V curves; the latter region is attributed to space charge, and dependent on measuring ambient. Bulk and surface resistances don't depend on ambient, indicating that the SCLC ambient sensitivity is an interfacial effect. Neither resistivity nor dielectric constant depend on sample thickness.

The leakage current setup was automated, using an IBM PC-XT computer, Keithley 705 scanner and 617 electrometer, and Okidata printer.

1. INTRODUCTION

The main goal of this program is to clarify fundamental (intrinsic) conduction mechanisms that exist in high-K ceramic and to relate these to MLC capacitor degradation.

Over this reporting period we have measured commercial capacitors and capacitor ceramic supplied by Corning Electronics, and some BaTiO₃ discs supplied by Penn State. For these samples we have attempted to clarify the nature of the charge carrier (using Galvanic cell measurements), the role of grain boundaries (modelling and impedance-frequency measurements), and the electrode-ceramic interface. The dependence of leakage current on time, the nature of the activation energy, and dielectric thickness are also discussed.

2. NATURE OF LEAKAGE CURRENT

a) Charge Carrier

Since the main signature of MLC capacitor degradation is increased leakage current, we should know as such as possible about the nature of that current and what causes it to increase with time under temperature, voltage and other stress.

Electrical conductivity σ is generally written as

$$\sigma = \sum_i q_i \mu_i N_i \quad (1)$$

We should start by asking: What are the N_i for a typical BaTiO₃ based ceramic? (Mobility will be addressed later.) The N_i can be electrons, holes and ions (cations, anions, vacancies). For an n-type solid, the main carrier is usually the electron. However, for certain BaTiO₃ based material, due mainly to the known movement of oxygen, and the often-seen 1.3eV activation energy, the oxygen vacancy is assumed to be the current carrier. (See ref. 1, for example, related to commercial Z5U devices).

We have verified that for a commercial BaTiO₃ based ceramic (X7R specification)*, the charge carrier responsible for current is the electron. This conclusion was arrived at by conducting several measurements on this ceramic, some of which have been discussed in earlier annual reports⁽²⁾. The principal techniques are thermoelectric (which verified that the carriers are negative), and Galvanic, which verified that the carrier is not oxygen (or oxygen vacancies.) These measurements were supplemented by measurements of leakage current dependence on time, temperature and voltage, all of which are consistent with the electron carrier model.

* Supplied by Corning Electronics

The thermoelectric (Seebeck) measurements were already reported in detail^(2,3). The reproducibly negative and stable voltages generated verify that the mobile charge carrier is negative, and of constant concentration over the time of measurement.

It should be noted that a negative Seebeck voltage can be generated in a p-type sample with ambipolar conduction, if hole mobility is much less than that of the electron⁽⁴⁾. We do not feel that such is the case here, although it is not an impossibility.*

The true test of ionic motion in a solid is mass transfer. If there is considerable movement of oxygen and oxygen vacancies in BaTiO₃ based material (so as to make a contribution to equation 1), this should be detectable in a Galvanic cell setup.

Such a setup was assembled; a schematic is shown in Figure 1^(5,6). Two quartz tubes were mounted vertically in a tube furnace (Thermolyne Type 21100). Different oxygen partial pressures were maintained in the two tubes, between which a given sample is clamped. Samples were all about 1cm. dia and 0.5-1mm thickness, with Pt electrodes (Engelhard Type 6926-unfluxed). A disc of single crystal Y₂O₃ modified ZrO₂ (9.4M%Y₂O₃) was used as an ion-conducting reference. BaTiO₃ ceramic discs obtained from Penn State, and some commercial BaTiO₃ based blanks obtained from Corning electronics were measured.

Results are shown in Figure 2. The ZrO₂ disc generates a voltage nearly equal to that predicted by the equation

$$V = \frac{RT}{4F} \ln\left(\frac{PO''_2}{PO'_2}\right) \quad (2)$$

which is represented by the solid line in Figure 2. Experimental voltages may be a little low for the ZrO₂ because temperatures are also less than those where ZrO₂ is normally used for oxygen sensing⁽⁷⁾.

No measurable voltage was detected in any of the BaTiO₃ based samples, over the temperature range 500-800°C. (Four discs from Penn State and two X7R types from Corning were measured). Oxygen diffusion does not directly contribute to current at these temperatures, and probably not at lower temperatures (i.e. near room temperature)⁽⁷⁾.

The 1-1.3eV activation energy often measured for BaTiO₃ based materials^(1-3,8) must be attributed to electronic processes rather than ionic, unless those samples are in a totally different regime

* This is a rather moot issue, since electrons will still dominate the conduction, and the solid will be effectively n-type.

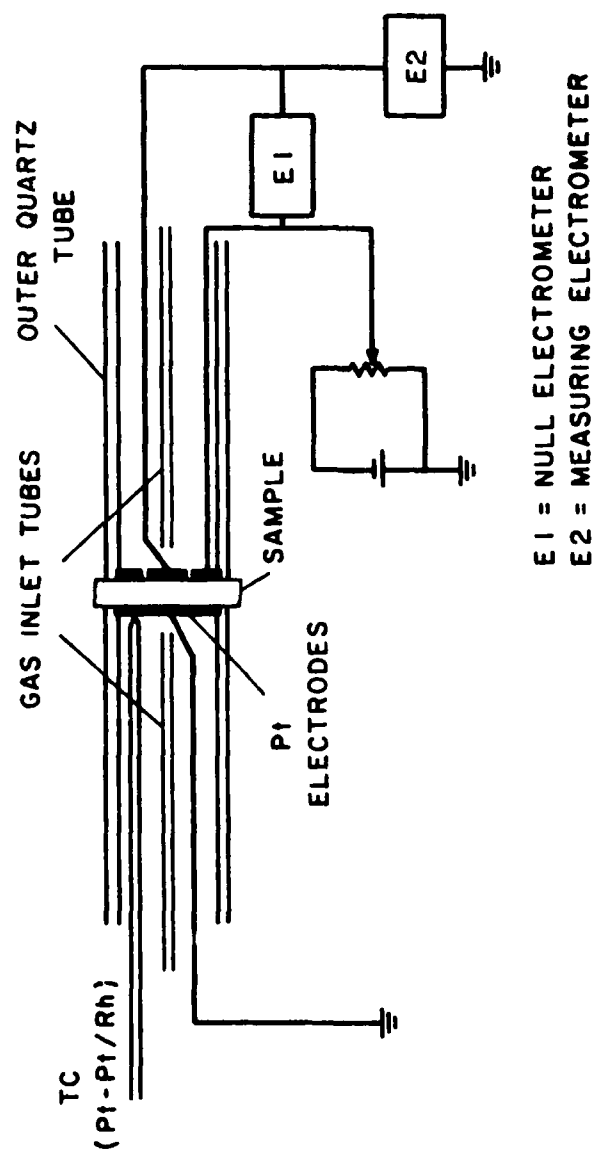


Figure 1. Schematic of Galvanic cell setup.

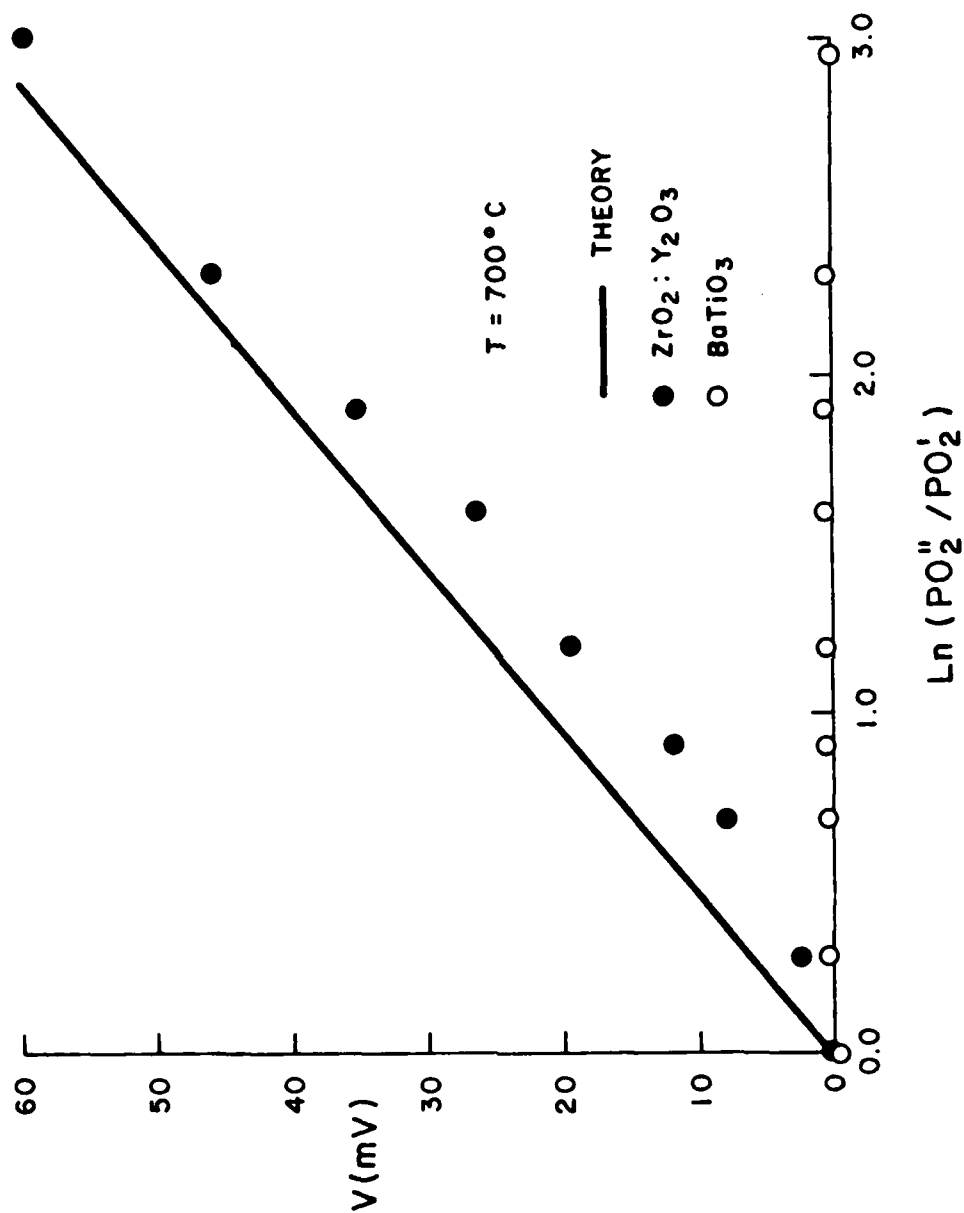


Figure 2. Galvanic cell voltage versus oxygen pressure ratio for yttria stabilized zirconia and BaTiO_3 .

That ions are not the main current carriers is also substantiated by leakage current measurements versus time and voltage. For example, Figure 3 shows current vs time for a commercial X7R device under increasingly severe stress over a period of 80 days. Note the constancy of the leakage current in all cases. (This is typical of good devices, prior to degradation/failure.) Even at 8x rated voltage and 170°C, the current is stable for 30 days (end of test.) If even a minor fraction of the current were due to oxygen migration, the current would increase due to the increased number of conduction electrons. (See model later in this section).

There have been many reports of space charge limited currents (SCLC) in BaTiO₃ materials⁽¹⁰⁾, and MLC capacitors^(2,3,8). Even though ionic SCLC has been reported⁽⁹⁾, we do not feel that the SCLC seen in the BaTiO₃ materials is ionic because there would have to be a steady supply of ions (O²⁻) supplied by the cathode. It is much more likely that the SCLC is electronic, especially in view of the Galvanic measurements discussed earlier.

Even though the leakage current is electronic, it is enhanced by oxygen migration as expressed by the equation



whereby 2 conduction electrons are generated per ion. The electron concentration n in an MLC device under stress therefore consists of two parts, $n = n_1 + n_2$, where n_1 is due to impurities and other donors in the as-made material, and n_2 is due to oxygen vacancies generated under stress, i.e. $n_2 = 2[V_O^{\bullet\bullet}]$. Then, in the ohmic region, conductivity is given by $\sigma = q \mu_e (n_1 + n_2)$ where μ_e is electron mobility. Even though donor impurities may move, segregate and change n_1 , the main time dependent effect will be an increase in n_2 (μ_e will also increase with time⁽³⁾, due possibly to grain boundary barrier height reduction - which is the case for the ZnO varistor⁽¹¹⁾, - or other causes).

Thus the current-time relation for an MLC capacitor can be represented generically as shown in Figure 4. In region I, conduction is governed by n_1 , in region II by n_2 , with failure occurring in region III. Several comments can be made about the shape of this curve. a) The time scale depends on temperature, voltage stress and type of device. This is indicated in Figure 5, where the time scale shortens with increasing stress. b) The initial decrease in current may extend over a long time period, prior to degradation. (This is a decreasing steady - state current; not the initial transient that is always seen when bias voltage is applied or increased). Such a decrease may be due to depolarization, to impurity migration, or to high field

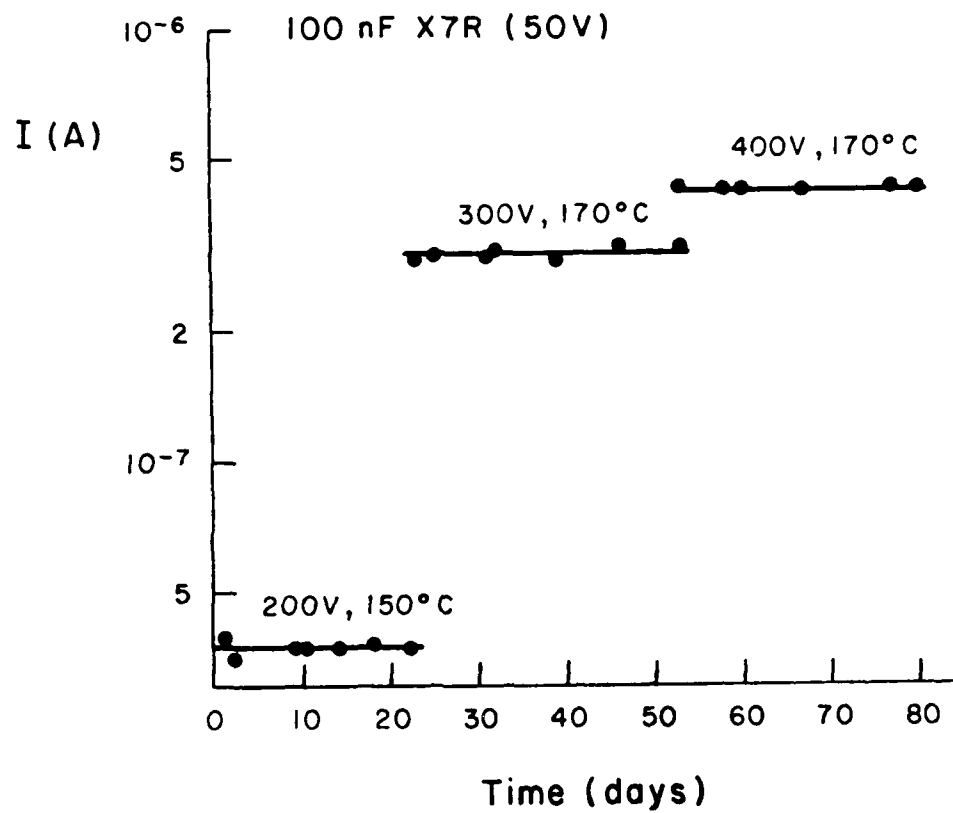


Figure 3. Leakage current versus time for X7R MLC capacitor at three stress levels (Corresponds to region I of Figure 4).

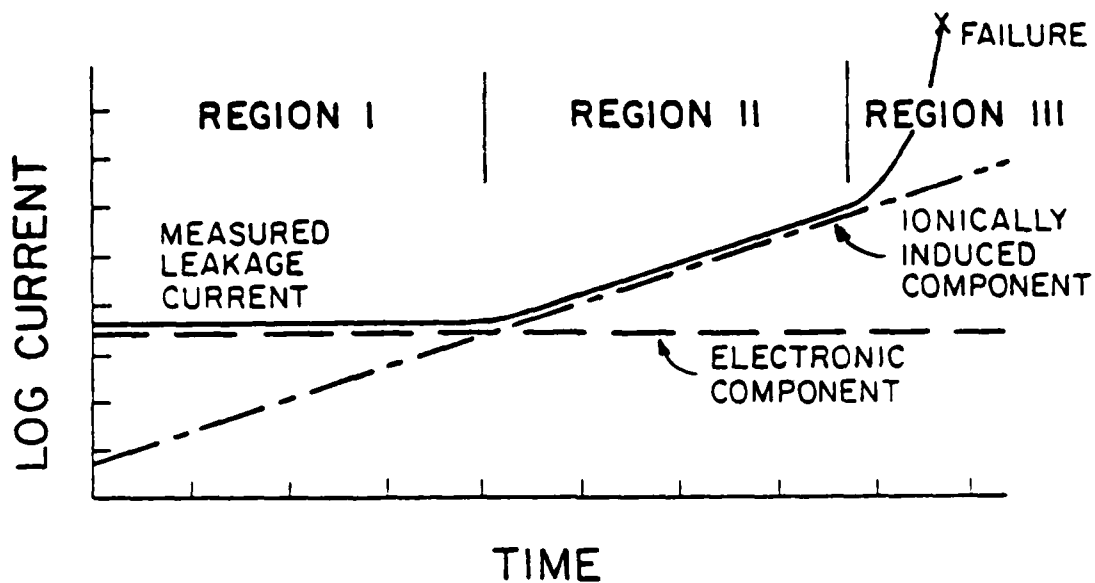


Figure 4. Generic plot of leakage current versus time.

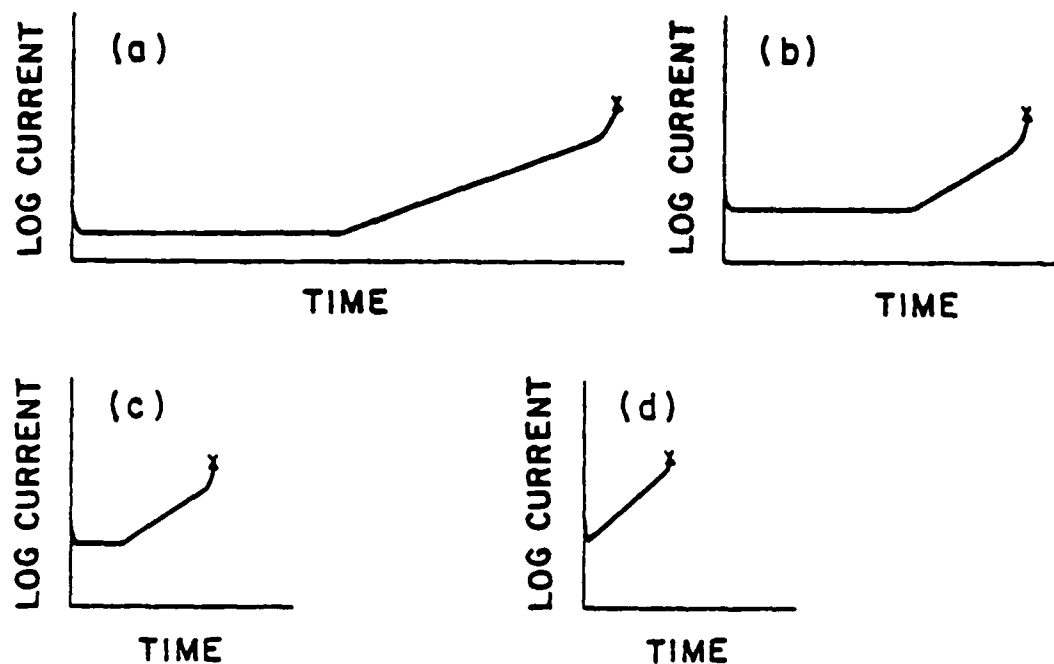


Figure 5. Leakage current versus time as temperature and/or voltage increase (a to d).

neutralization due to charge trapping⁽¹²⁾, c) In region II, the current is often seen to increase roughly exponentially with time. We reported such an exponential time dependence for an X7R device in last year's report⁽²⁾, for high-K thick film capacitors⁽¹³⁾, and for commercial Z5U devices^(2,14). There are at least two independent models that can account for exponentially increasing leaking currents with time.

Model 1

One model for an exponentially increasing leakage current with time is based on the following assumptions:

- (i) Current is proportional to conduction electron density;
- (ii) Conduction electrons are due to oxygen vacancies.
- (iii) There is no supply of oxygen to replenish that which leaves.

For a sample of cross section A and thickness W, oxygen vacancy current I_{ion} can be expressed in two forms:

$$I_{ion} = 2qWAd[V_0]/dt \quad (4)$$

and

$$I_{ion} = 2qA\mu_i \frac{V_0}{W} [V_0] \quad (5)$$

where μ_i = ion mobility, V = applied voltage, and the electric field is assumed uniform at V/W. These equations give

$$d \frac{[V_0]}{dt} = \mu_i \frac{V}{W^2} [V_0] \quad (6)$$

Or, since we are assuming $n_e = 2[V_0]$

$$\frac{dn_e}{dt} = \mu_i \frac{V}{W^2} n_e \quad (7)$$

where n_e is conduction electron concentration. This integrates to

$$n_e(t) = n_e(0)e^{\beta t}, \quad \beta = \frac{\mu_i V}{2W^2} \quad (8)$$

Leakage current conductivity σ can thus be expressed (in ohmic regime)

$$\sigma(t) = q\mu_e n_e(t) e^{\beta t} \quad (9)$$

The degradation time constant β depends on three important parameters: varying directly with ion mobility and applied voltage, and inversely with W^2 . It appears that one could estimate ion mobility from a slope of the $\ln \sigma$ vs t curve, but this neglects the fact that μ_e is also changing with time, perhaps as much as $n_e^{(3)}$ (i.e. the experimental β is not the same as the β in the above equation).

Model 2

A second model is based on a reduction of the grain boundary (GB) barrier height with time. If carrier flow is limited by transport across GB potential barriers, current can be expressed as I is proportional to $e^{-\phi_B/kT}$ where ϕ_B is GB barrier height. For uniform grains, $\phi_B \propto Q_{GB}^2$ where Q_{GB} is negative charge trapped at the GB and N_D is donor density in the grains. Assume that N_D is constant and Q_{GB} decreases linearly with time due to a flux of positive ions into the GB. Q_{GB} would then reduce to $Q_{GB}(0)(1 - \alpha t)$ and $Q_{GB}^2 \sim Q_{GB}^2(0)(1 - 2\alpha t)$ for $\alpha t < 1$. ϕ_B would thus decrease linearly with time, and current would go as

$$I \propto e^{-\phi_B/kT} = e^{\gamma t}, \quad \gamma = \text{constant} \quad (10)$$

This model is physically attractive if GB potentials exist, because the field near the GB would tend to attract positive ions toward the GB on both sides. (A similar model has been used to account for ZnO varistor degradation due to transport of Zn^{+2} toward the GB, thus depleting the space charge region⁽¹¹⁾. It should also be noted, on the other hand, that oxygen ions would be repelled from the GB region, and their diffusion across the ceramic would overall be inhibited (although they may diffuse along grain boundaries.)

If these two exponential or near-exponential processes are both occurring (reduction of a potential barrier which would increase mobility, and increase of electron concentration), then the overall effect will also appear exponential with time.

These arguments can be reversed, and exponential decreases in leakage current predicted. The above two models would both go in this direction if donors were diffusing out of the ceramic, reducing n_e , or ϕ_B was increasing due to increased Q_{GB} or decreased N_D . We have reported such a decrease in leakage current. (p. 37 of 1985 Annual Report).

b) Activation Energy (E_A)

Now that the carrier has been identified (at least in the X7R material we have measured), something should be said about the mode of transport, often characterized by an activation energy. For X7R ceramic and MLC capacitors we have measured, activation energies have several characteristics:

- (i) Values for as-made samples/devices are often in the 1.0-1.3 eV range;
- (ii) Values drop to near zero with degradation under voltage/temperature stress^(2,3).
- (iii) E_A is constant from 150°C to 600° (the range of measurement - see Figure 6)
- (iv) E_A values are independent of bias voltage for X7R, although decrease with increasing voltage for Z5U and NPO;⁽¹⁸⁾.
- (v) Thermoelectric measurements indicate that E_A can be attributed almost entirely to transport (i.e. mobility) as contrasted to thermal activation of charge carriers, especially for degraded (reduced) ceramic⁽³⁾.

There are at least four physical mechanisms to which a 1.3 eV activation energy may be attributed, in this case: oxygen ion diffusion, polaron hopping transport, grain boundary barrier transport, and thermal activation of a deep donor. Oxygen diffusion is ruled out because it is not the charge carrier for current, as was discussed earlier. Deep donor activation is unlikely, judging from our thermo-electric measurements (where n is essentially constant with temperature). This leaves transport (polaron and grain boundary). Even though impedance measurements indicate there may be GB impedance (discussed later), this is still an unresolved issue. Assuming GB and polarons have different activation energies, this should be evident when single crystal BaTiO₃ is compared to ceramic. But their activation energies are similar. Maybe polarons and GB transmission have similar E_A (see Figure 19). How else should GB impedance be evident? One would expect a GB activation energy to decrease at high fields; E_A for X7R devices do not. If E_A for polarons and GB are similar, the I-V would become super-ohmic if the GB collapsed as V increased, but E_A would remain the same as polarons took over. This is roughly what happens for X7R. (The GB collapse would not be seen in capacitance, because GB capacitance would be so much larger than that of the grains, and they are in series). Also if GB impedance is present, and disappears at some high voltage, one would expect a linear I-V to ensue. This may be an explanation for the very interesting result shown in Figure 7, for an X7R device, where the I-V curve becomes linear above roughly twice rated voltage.

Thus it appears that polaron and GB transport may exist together in the types of X7R we have measured. How then does one account for the decrease in E_A resulting from degradation? One way is a

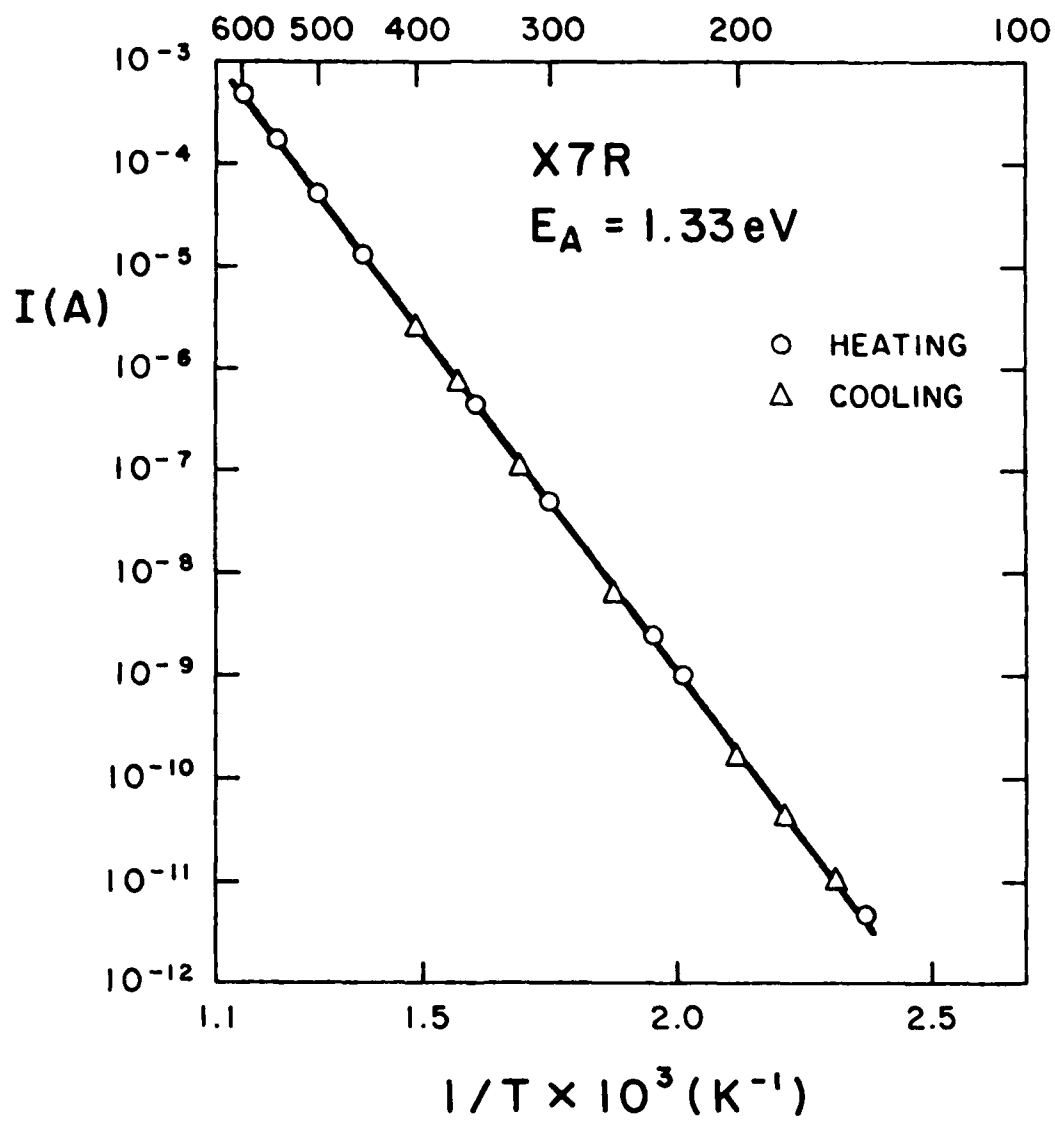


Figure 6. Leakage current versus $1/T$ for X7R capacitor chip, from 150-600°C.

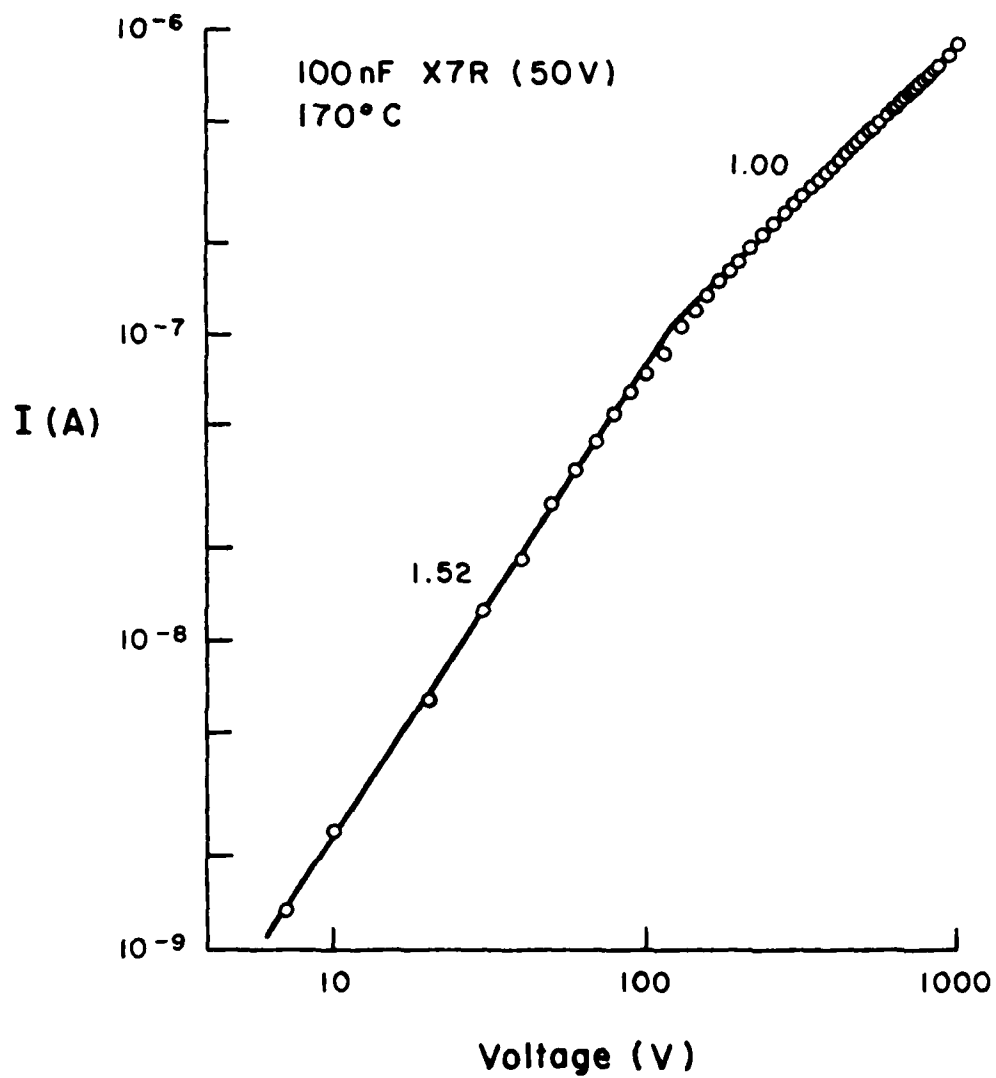


Figure 7. Current versus voltage for X7R MLC capacitor, showing high voltage ohmic region.

reduction of the GB potential barrier with time. A second (and even perhaps concurrent) reduction in E_A could be due to a reduced polaron hopping potential. This might be caused by screening of the conduction electrons (polarons) by other electrons and oxygen vacancies if the latter concentrations get large enough⁽²⁸⁾. $|E_s|$ would be reduced by an amount⁽²⁾.

$$\Delta E_A = \frac{-q^2}{4\pi\epsilon\lambda} \quad (11)$$

where λ is the Debye length.* For electron concentration of 10^{18} cm^{-3} and $\epsilon = 100\epsilon_0$, $|\Delta E_A| < 0.01 \text{ eV}$, which is insignificant.

3. ROLE OF GRAIN BOUNDARIES

Grain boundaries (GB) play such a dominant role in a variety of polycrystalline devices and materials (varistor, thermistor, barrier layer capacitor, poly-Si, thin films, thick films, etc.) that it should be established what their role is in high resistance/high-K ceramic. In this light, first some models will be discussed, then some measurements.

a) GB Modelling

It is feasible to start with the same type of model used for poly-Si⁽¹⁵⁾, the ZnO varistor⁽¹⁶⁾ and other low K, semiconducting materials. In applying such a model to higher K, high resistance and often inhomogeneous materials, we have made several assumptions:

- (i) Grains and GB are homogeneous and uniform. It is known that for certain types of MLC capacitor ceramic this is not true. Rawal and Kahn have reported relatively impurity free grain cores of tetragonal BaTiO₃ surrounded by heavy donor doped, cubic shells, for grain-growth-inhibited BaTiO₃⁽¹⁷⁾. However, GB potential barriers could still exist, even though modified by the higher donor dopant concentration. Since the electrically active donor concentration is pretty much an unknown in any case, such inhomogeneity as noted above does not significantly alter the GB charge trapping, which controls GB impedance. In this regard, properties of the GB itself are more important than inhomogeneities, even though the latter will alter the conduction band shape (ref. 18, Fig. 2).

* Assuming classical statistics. The above conclusions don't change significantly if the polaron gas becomes degenerate.

- (ii) Charge due to the polarization discontinuity between grains is neglected. As is thought to be the case for BaTiO₃ based thermistors, the effect of this charge below the Curie temperature should be to compensate roughly half of the trapped GB charge, thus lowering the overall resistance⁽¹⁹⁾. Neglect of this charge will thus result in estimated overall GB resistance that will be on the high side.
- (iii) The GB potential barrier is due to trapped electrons and associated positive space charge;
- (iv) The GB itself is infinitesimally thin, with no second phase or other material present (with the possible exception of excess oxygen and dopant atoms).

Thus even though these assumptions are to varying degrees untrue (especially the first two), some conclusions can still be obtained that are general enough to be valid for high K, high resistance ceramic.

A GB potential barrier is shown in Figure 8. Electrons of total charge $Q_{GB} = qN_{GB}$ per cm² are trapped below the Fermi level, where N_{GB} is the GB trap density. The GB resistance can be expressed as $R_{GB} \propto e^{\phi_B/kT}$, which says essentially that only those conduction electrons with energy above ϕ_B can be thermally emitted over the barrier.

The barrier height ϕ_B can be written as

$$\phi_B = \frac{qN_D W^2}{2\epsilon} = \frac{Q_{GB}^2}{8q\epsilon N_D} \quad (12)$$

using the fact that $Q_{GB} = 2qWN_D$ from charge neutrality. The important materials parameters that influence ϕ_B are donor density and dielectric constant.

For given GB trap density and dielectric constant, GB resistance is determined by N_D and grain size. There are two regimes of interest. If $W < D/2$ (D = grain diameter), the depletion layer extends less than half-way across the grain. ϕ_B is then given by eq. 12. However, as N_D and/or D decrease, there may not be enough charge in the grain (i.e. conduction electrons) to compensate GB charge Q_{GB} . Then Q_{GB} decreases, and ϕ_B is reduced to the value

$$\phi_B = \frac{qN_D(D/2)^2}{2\epsilon} \quad (13)$$

This result can be proven by integrating Poisson's equation twice

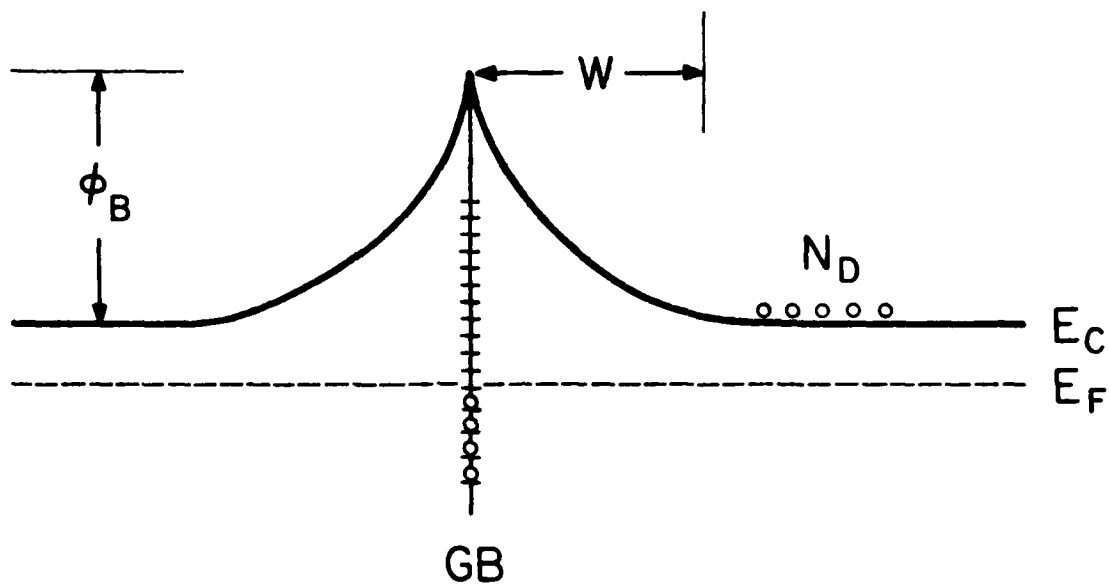


Figure 8. Grain boundary potential energy barrier.

$$\frac{d^2 V}{dx^2} = \frac{qN_D}{\epsilon} \quad (14)$$

with boundary conditions $dV/dx = V = 0$ at $X = D/2$ ($x = 0$ at GB). The result for potential in the grain is

$$V(x) = \frac{qN_D}{2\epsilon} \left(\frac{D}{2} - x \right)^2, \quad |x| < \frac{D}{2} \quad (15)$$

At $x = 0$, $V = \phi_B = \frac{qN_D(D/2)^2}{2\epsilon}$ which verifies (13). This can be compared to the value for large grains ($W < D/2$, eqn.12). The ratio is

$$\frac{\phi_B(W > D/2)}{\phi_B(W < D/2)} = \left(\frac{D}{2W} \right)^2 \quad (16)$$

As an example, for $N_D = 10^{15}$, W would be $10\mu\text{m}$ if D were $> 20\mu\text{m}$. But if D is say $1\mu\text{m}$, the grains are totally depleted and ϕ_B is reduced to less than 1% of its large grain value.

The two regimes of grain size are evident in Figure 9, with other parameters indicated. Grains smaller than $1\mu\text{m}$ (for this example) are totally depleted, and barrier height falls accordingly.

Another interesting situation can be seen by comparing equations 12 (undepleted grains) and 13 (depleted grains). In these equations, ϕ_B varies linearly and inversely with N_D . This means that for a given grain size, ϕ_B decreases for small or large donor concentrations, as shown in Figure 10. In this figure, ϕ_B was determined for $D = 1\mu\text{m}$, $K = 100$, and $N_{GB} = 10^{13}\text{cm}^{-2}$. It is seen that for N_D outside of the $10^{16} - 10^{19}\text{cm}^{-3}$ range, ϕ_B is less than about 0.1eV, i.e. not very important.

This flatness of the conduction band at low and high carrier concentration, with a peaking in between, is illustrated in Figure 11.

In all of these examples, dielectric constant of 100 was assumed. If K is in the range 2,000-8,000, such as for X7R or Z5U capacitors, ϕ_B would be reduced by a factor of 20-80, which is substantial. Of course, this decrease due to high K could be balanced by larger N_{GB} , since $\phi_B \propto N_{GB}^2$. One mechanism could be excess oxygen atoms at the GB, each of which would contribute two electron traps toward N_{GB} .

We have discussed current flow across GB, and the voltage division between grain and GB, in published papers^(18,20). In summary, a ceramic GB should influence current in the same way as for

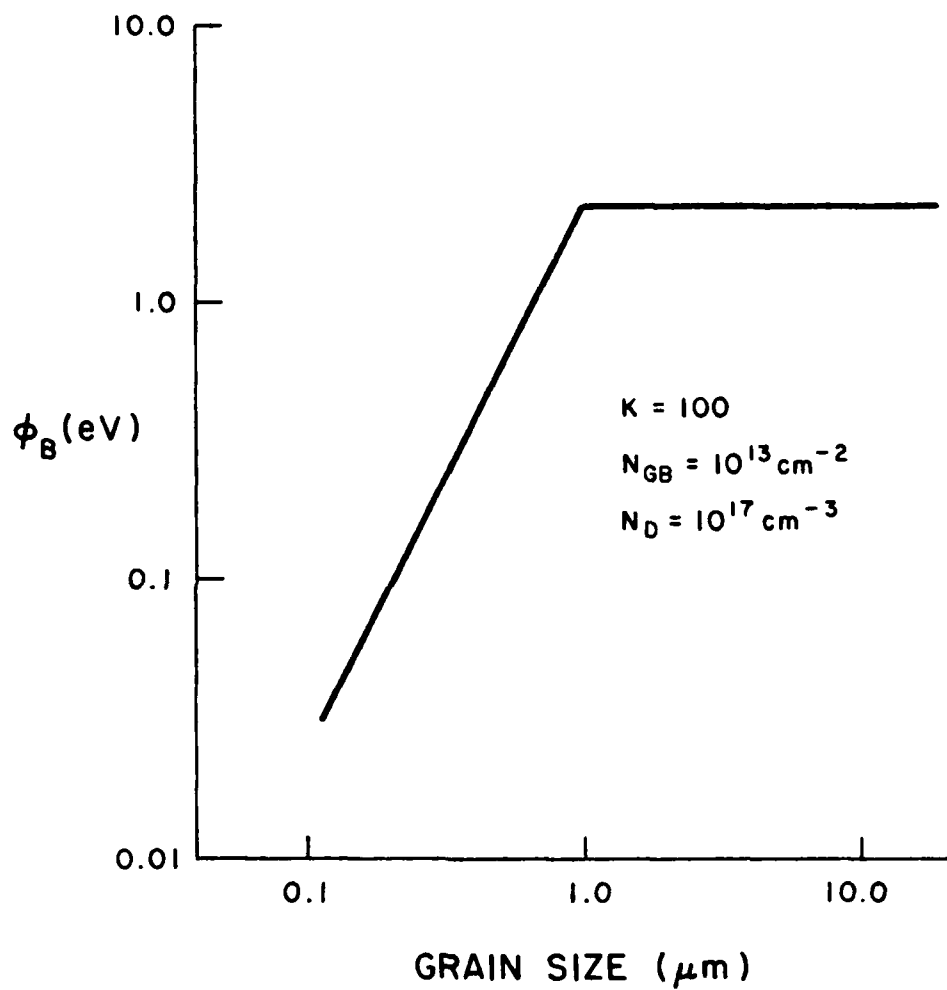
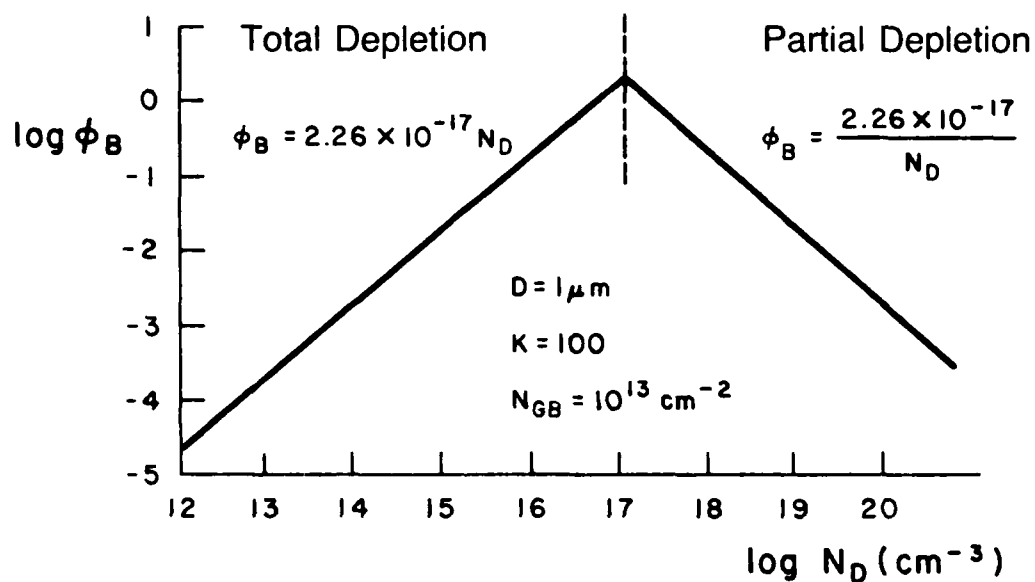


Figure 9. Dependence of grain boundary barrier height on grain size; other parameters indicated.

GRAIN BOUNDARY BARRIER ϕ_B



ϕ_B = Barrier height

D = Grain dia.

N_D = Donor density in grain

N_{GB} = Grain boundary state density

Figure 10. Dependence of grain boundary barrier height on donor density; other parameters indicated.

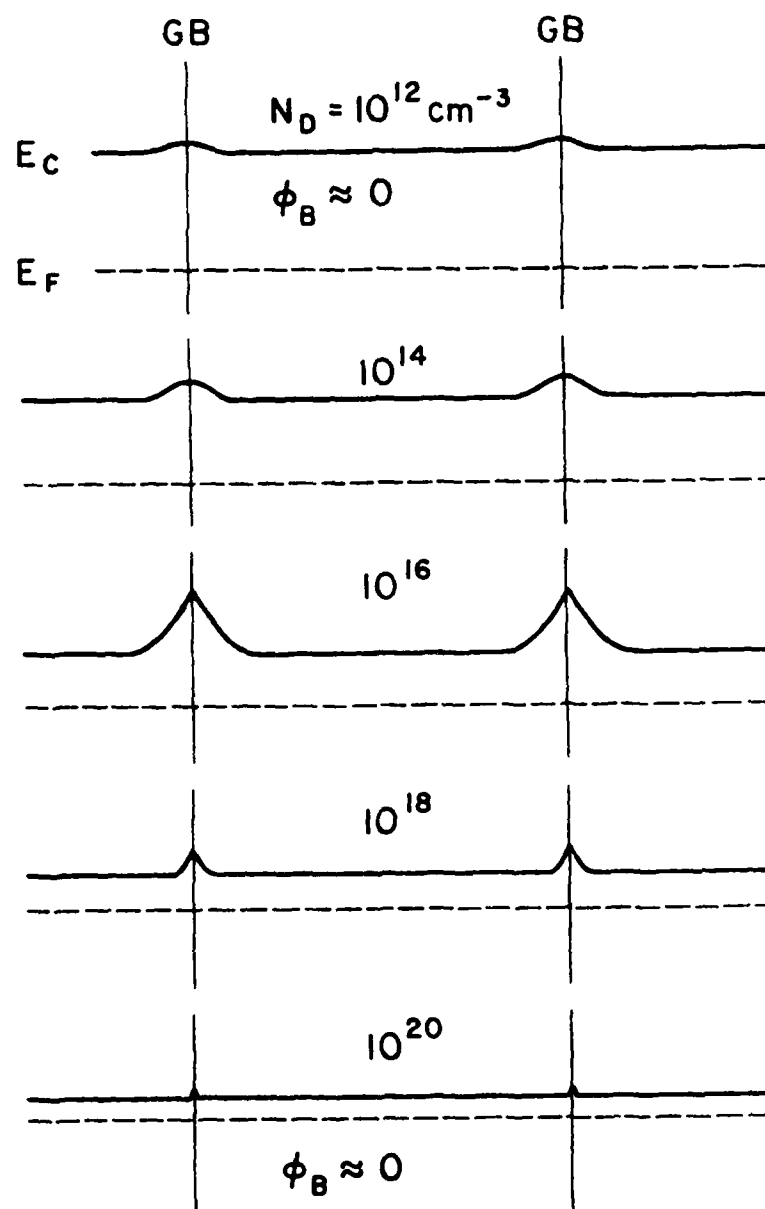


Figure 11. Variation of conduction band spike with donor density.

polycrystalline semiconductors, with the complication that a larger fraction is dropped across the grain itself. GB and grain voltage (V_{GB} and V_G) are related by⁽²⁰⁾ the relation

$$V_{GB} = \frac{kT}{q} \ln \left[1 - \frac{V_G}{R_G I_o} e^{(\phi_B + \eta)kT} \right] \quad (17)$$

where R_G is grain resistance, I_o is thermionic reverse current (viewing the GB as back-to-back Schottky diodes) and $\phi_B + \eta$ is distance from the Fermi energy to the top of the barrier height.

In last years report⁽²⁾, and in published form⁽¹⁸⁾ we have pointed out the similarity between the super-ohmic I-V behavior seen for MLC capacitors, and that of GB controlled devices such as varistors and poly-Si. It cannot be deduced directly from I-V curves, however, whether or not the MLC super ohmic nature is due to the collapse of a GB potential barrier with applied voltage⁽²¹⁾. (GB controlled semiconductors, such as poly-Si and BaTiO₃ PTC, are easier to model because their resistance is totally GB controlled; grain resistance is apparent only at very high current density).

Then one must ask: How can grain and GB resistances be experimentally identified? There are two ways that have been used for polycrystalline materials:

- (i) Place microprobes across a grain, and across a GB. This is feasible for large-grained material⁽²²⁾, but may be difficult for commercial X7R and COG ceramic, where grain sizes are less than a micron. Another possible problem for high resistance materials is the possibility of modified surface regions (surface leakage).
- (ii) Use of impedance - frequency measurements. This method has been used for some time on intermediate-resistance ceramic⁽²³⁾ (up to 1M Ω), and may be viable for bulk parameters of high-resistance ceramic. This method is discussed next.

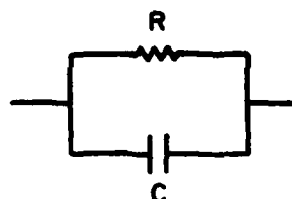
b) Impedance-Frequency Measurements

Complex impedance ($Z = Z' + jZ''$) or admittance ($Y = 1/Z$) measurements have been used to separate internal resistance contributions of polycrystalline materials, along the lines originally reported by Bauerle⁽²³⁾. Extensive measurements have been reported for intermediate resistance solids, such as yttria-modified zirconia^(23,24).

The method is based on the fact that an R-C network produces a semicircle in the negative half of the complex impedance plane, as illustrated in Figure 12. This can be extended to two or more RC sections (Figure 13), with a distinct semicircle appearing for each R-C section if none of the RC time constants are

IMPEDANCE ANALYSIS

Case 1



$$Z = \frac{R}{1 + \omega^2 R^2 C^2} - j \frac{\omega R^2 C}{1 + \omega^2 R^2 C^2} \equiv Z' + jZ''$$

$$\left(Z' - \frac{R}{2}\right)^2 + (Z'')^2 = \left(\frac{R}{2}\right)^2$$

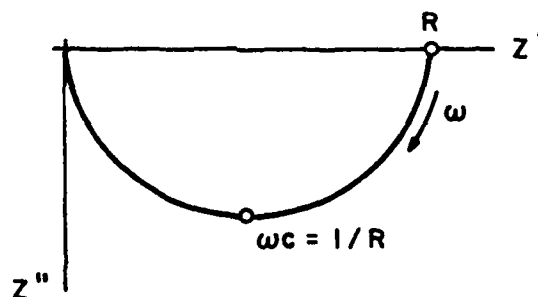
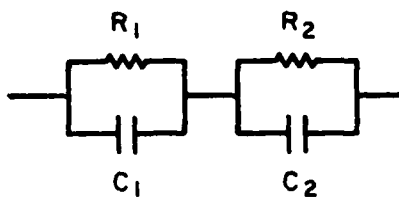
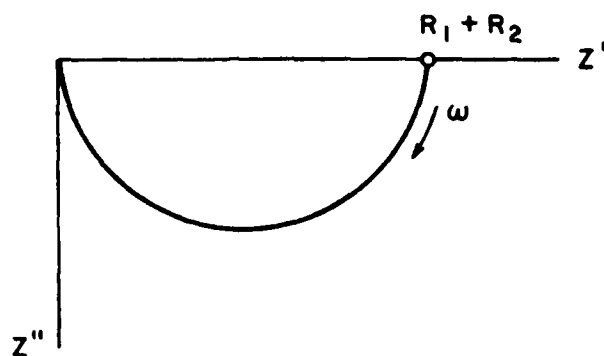


Figure 12. Impedance plot for single R-C network.

Case 2



a)



b)

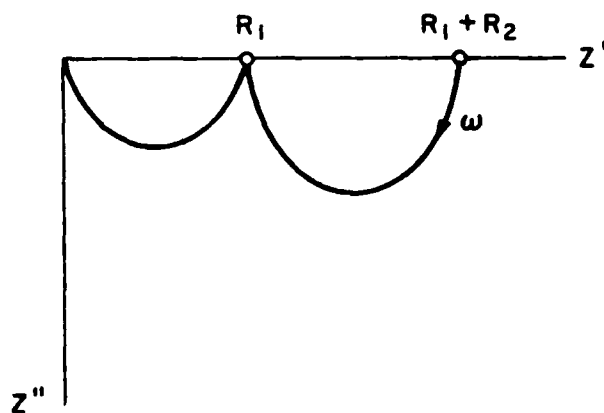


Figure 13. Impedance plots for 2-section R-C network; a) $R_1 C_1 = R_2 C_2$ b) $R_1 C_1 < R_2 C_2$.

close together. If the semicircles are distinct resistance values are determined from Z' intercepts, and capacitance values from the condition $\omega RC = 1$ at the minima, where ω is angular frequency.

There are several difficulties in applying this technique to high resistance ceramic:

- (i) If more than one semicircle exist, they are usually not distinct, but overlap, in an extreme case merging into one (nearly equal RC time constants). Interpretation then becomes more difficult⁽²⁵⁾.
- (ii) High resistance ceramic (which may be well over $10^{15}\Omega$ at room temperature, depending on geometry, etc.) must be heated in order to be measurable on most commercial bridges (a widely used impedance analyzer - the HP 4192A - has a upper limit of 1.3 M Ω).
- (iii) A lumped model may be inappropriate, since components of a given section may be distributed (due to non-uniform contacts, inhomogeneous GB, etc.)
- (iv) If the material is dispersive - i.e. R and/or C depend on frequency - the impedance plot will be modified, the amount depending on the degree of dispersion. Since most materials are dispersive to some degree, this ultimately has to be taken into account.

With these adversities in mind, we began impedance measurements in Fall 1985, on commercial NPO, X7R and Z5U ceramic from Corning, and into 1986 on those pieces and some BaTiO₃ discs from Penn State. We have also measured some commercial ZnO based varistors and some zirconia single crystals, since they are dominated by and free from grain boundaries, respectively. Measurement temperatures for these samples were dictated by sample resistance, as noted above, since an HP 4192A bridge was used.

Plots for a GE V18ZA1 varistor are shown in Figure 14, and for an yttria stabilized zirconia disc in Figure 15. The varistor semicircle is due to GB impedance alone. As suspected from the highly super-ohmic I-V curve for the varistor, the impedance semicircle can be collapsed by applying bias (this was also used to reduce varistor resistance so that measurement could be made at lower temperature; the Figure 14 curves were done at biases of 10 and 15 volts). There is no evidence of contact resistance on the varistor characteristic.

Such voltage biasing could be very important when applied to capacitor ceramic during impedance measurements, for modulation of a given R-C section, which would be evident on the impedance plot.

The zirconia plot shows two curves; the complete semicircle is attributed to the body, and the low frequency tail to contacts⁽²⁴⁾. (All samples had Pt electrodes).

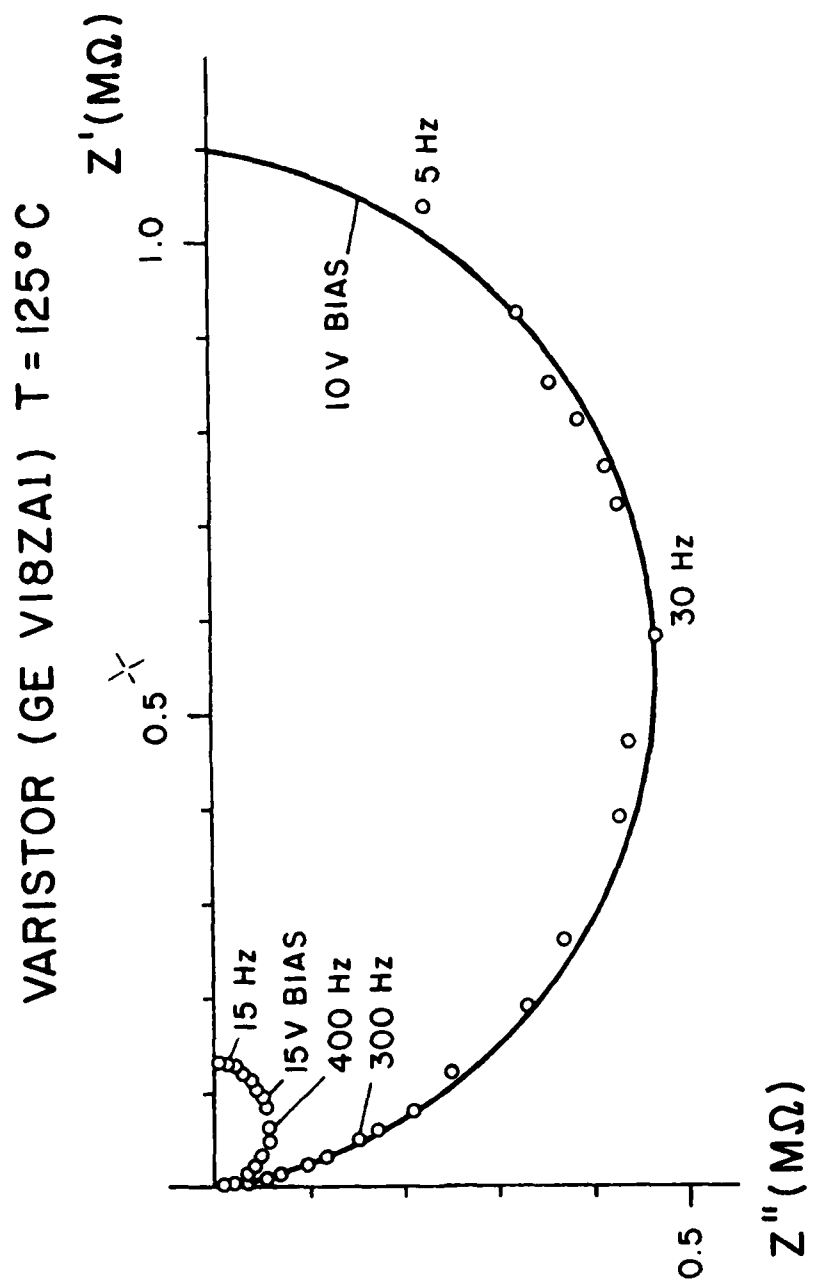


Figure 14. Impedance plots for commercial varistor at 10 and 15 volt biases.

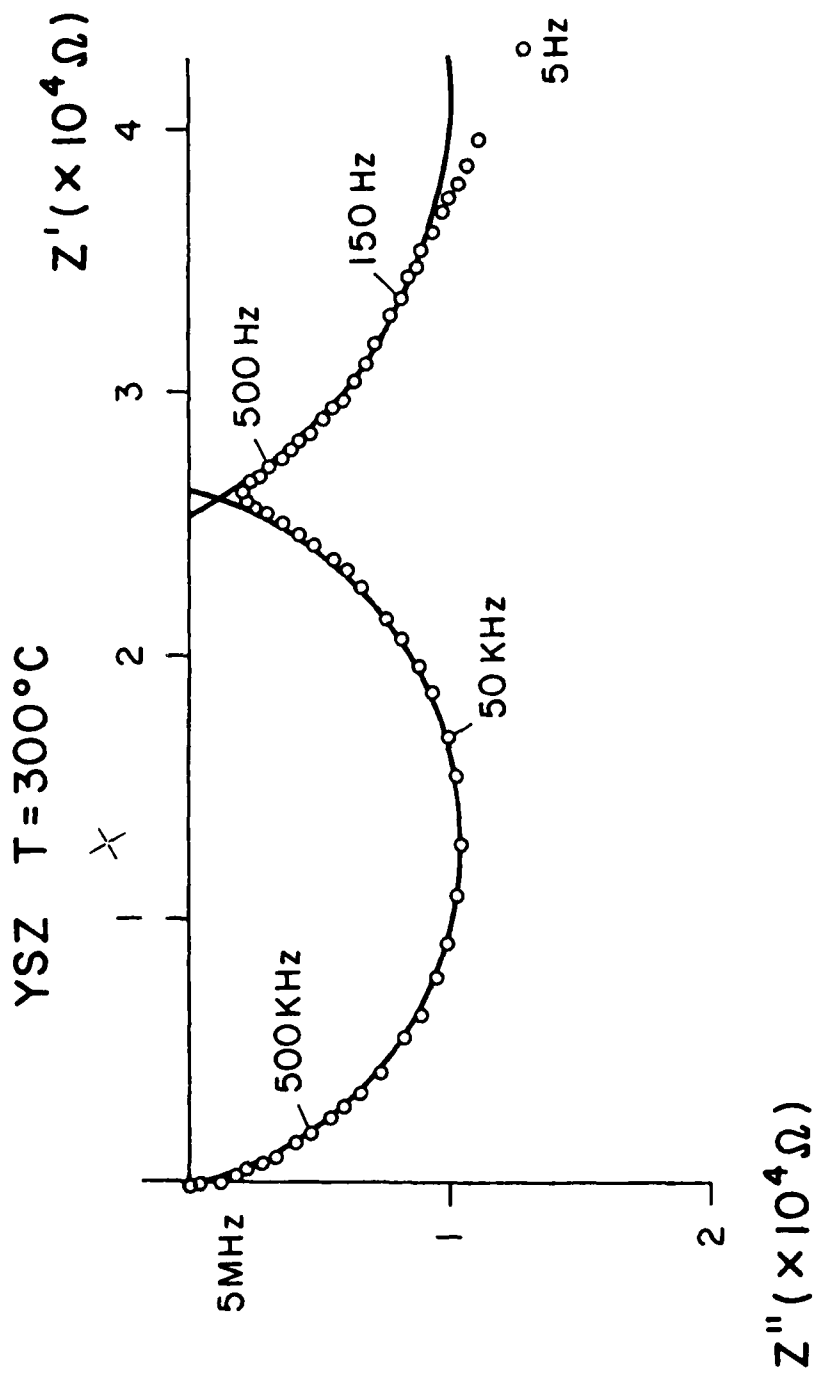


Figure 15. Impedance plot for single crystal yttria stabilized zirconia.

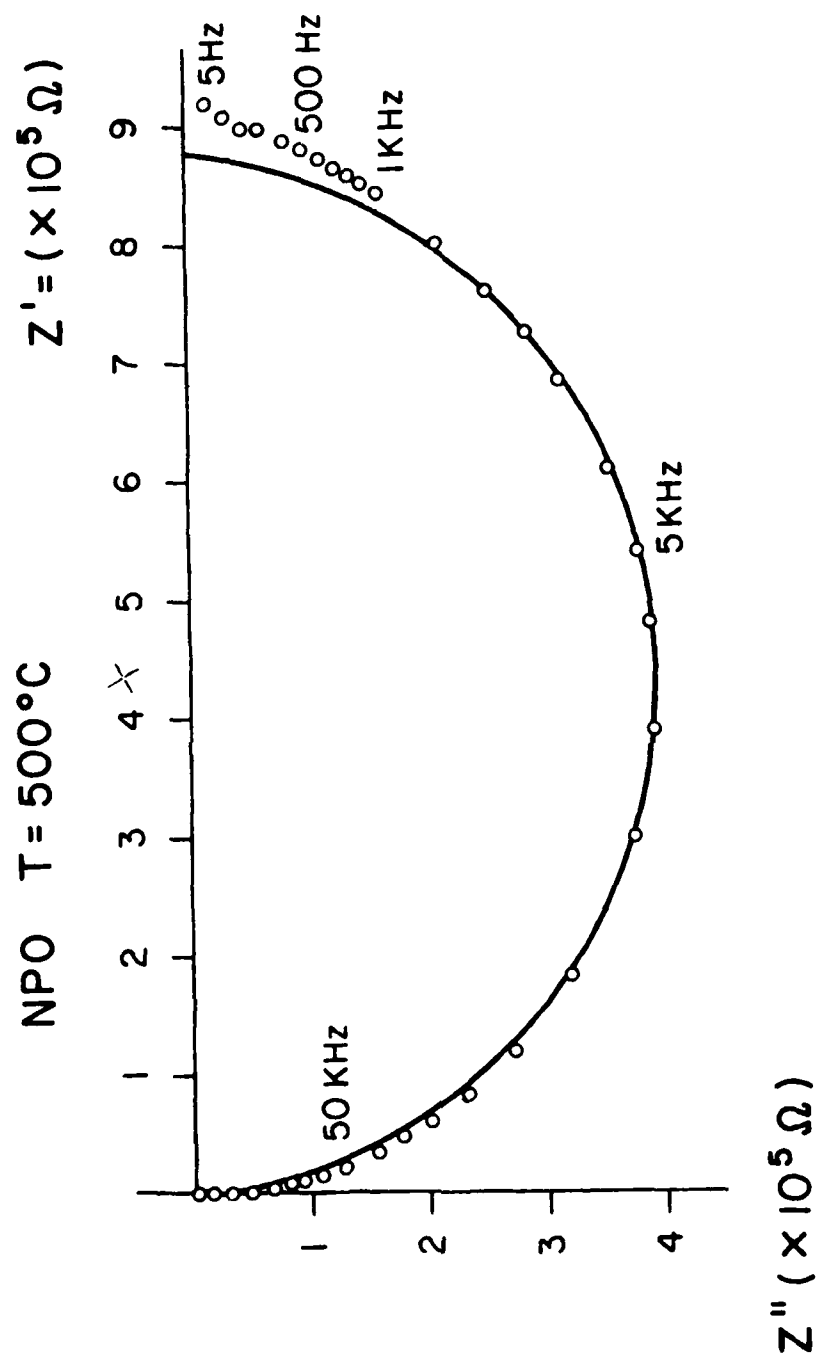


Figure 16. Impedance plot for commercial NPO capacitor ceramic.

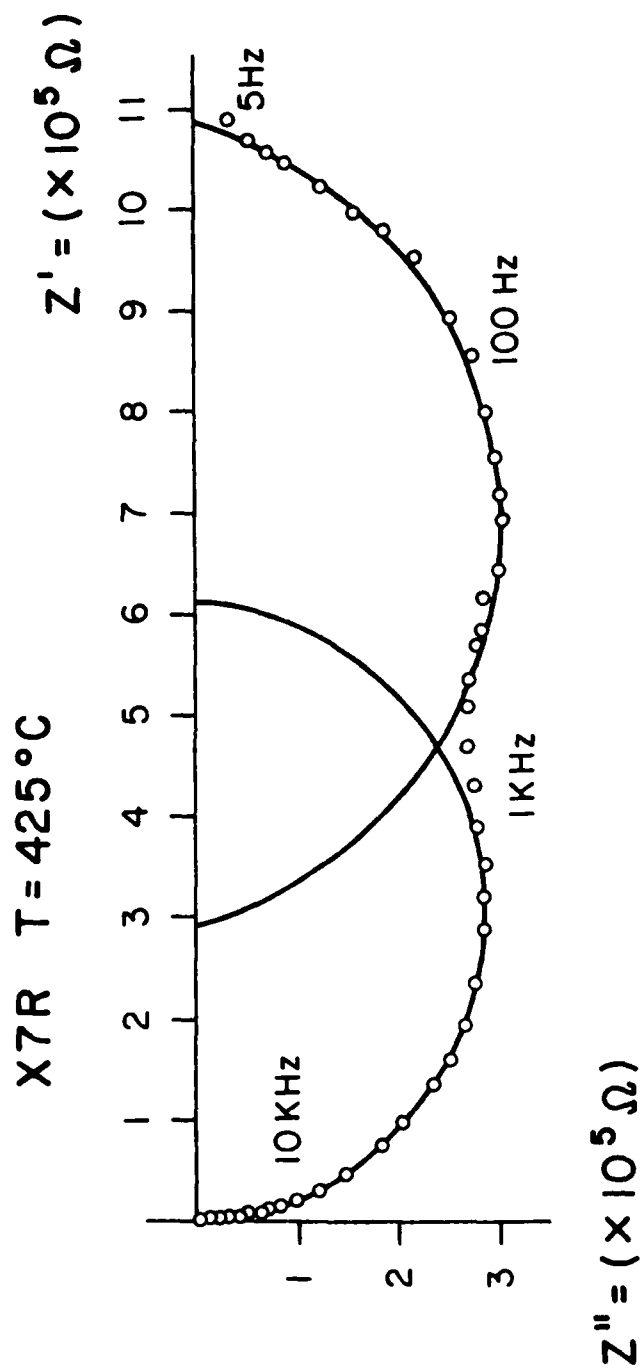


Figure 17. Impedance plot for commercial BaTiO_3 based X7R capacitor ceramic.

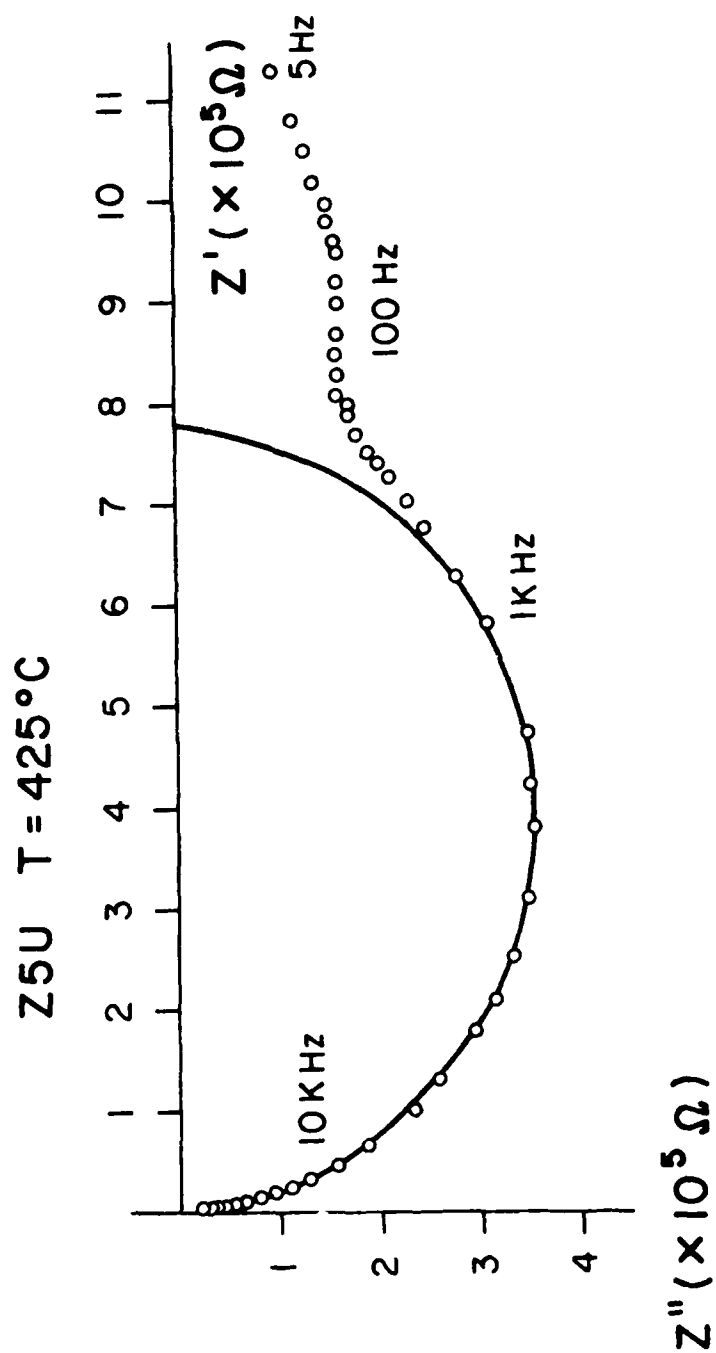


Figure 18. Impedance plot for commercial Z5U ceramic.

Figures 16-18 are for commercial BaTiO₃ based NPO, X7R and Z5U ceramic obtained from Corning Electronics, at indicated temperatures. (Runs made at other temperatures showed similar structure, as long as total resistance was below 1.3 MΩ). Two samples of each type were measured.

NPO samples gave approximate semicircles for all runs. There is no clear evidence of additional structure or contact effects on the low frequency side.

X7R samples exhibit two distinct semicircles for all temperatures. The upper frequency curve is attributed to the ceramic body; the lower frequency one could be due to either GB or contacts. Their contribution would appear at lower frequencies since their capacitance values would be larger (effective capacitive thicknesses much less than that of body).

Z5U samples also show some low frequency structure (Figure 18). The relative flatness of the low frequency curve could be due to non-uniform contact, which can't be represented by a single R-C section, but requires a larger number, which would flatten the overall curve.

The two resistance values deduced from Figure 17 (X7R), at different temperatures, have nearly equal thermal activation energies. (See Fig. 19). If the two circles do represent grains and GB, then a common mechanism might dominate grain and GB carrier concentration/transport. Further measurements (voltage biased impedance measurements, for example) will be needed to clarify this.

There is also evidence of impedance plot structure dependence on BaTiO₃ stoichiometry, as seen in Figs. 20 and 21, for Ba-deficient and Ba-rich discs. There is evidence of grain, GB and contact impedance for the Ba-rich disc at high, mid and low frequencies respectively. The Ba-deficient disc indicates only one impedance contribution. This difference could exist in part if the Ba-deficient disc is p-type, because of the high work function of the Pt electrodes, resulting in ohmic contacts. More detailed interpretation and comparison depends on such things as GB segregation, grain size, second phases, etc.

There are several recommendations that can be made for samples such as the above BaTiO₃ discs.

- a) Voltage bias, as noted earlier, could be used to modulate whichever parts are voltage sensitive; b) variation of grain size (with constant thickness) would change the grain to GB resistance ratio, which might be discernible in the impedance plot; c) variation of thickness (keeping grain size constant) would alter both the grain and GB resistances, but contact resistance should remain constant. Techniques such as these might be useful for separating and studying grain, GB and contact components of impedance.

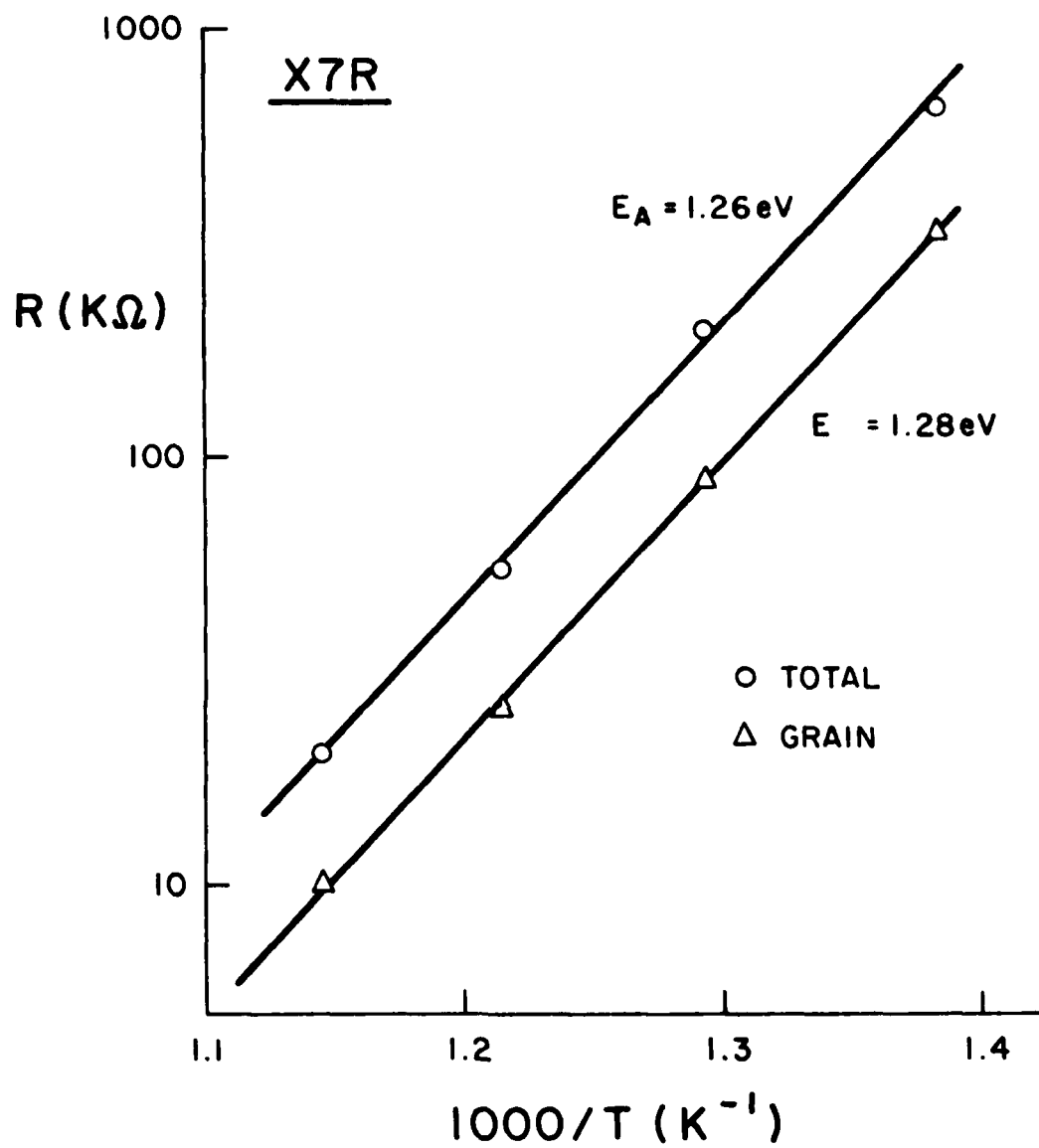


Figure 19. Total and grain resistances versus $1/T$ from impedance plots for X7R ceramic.

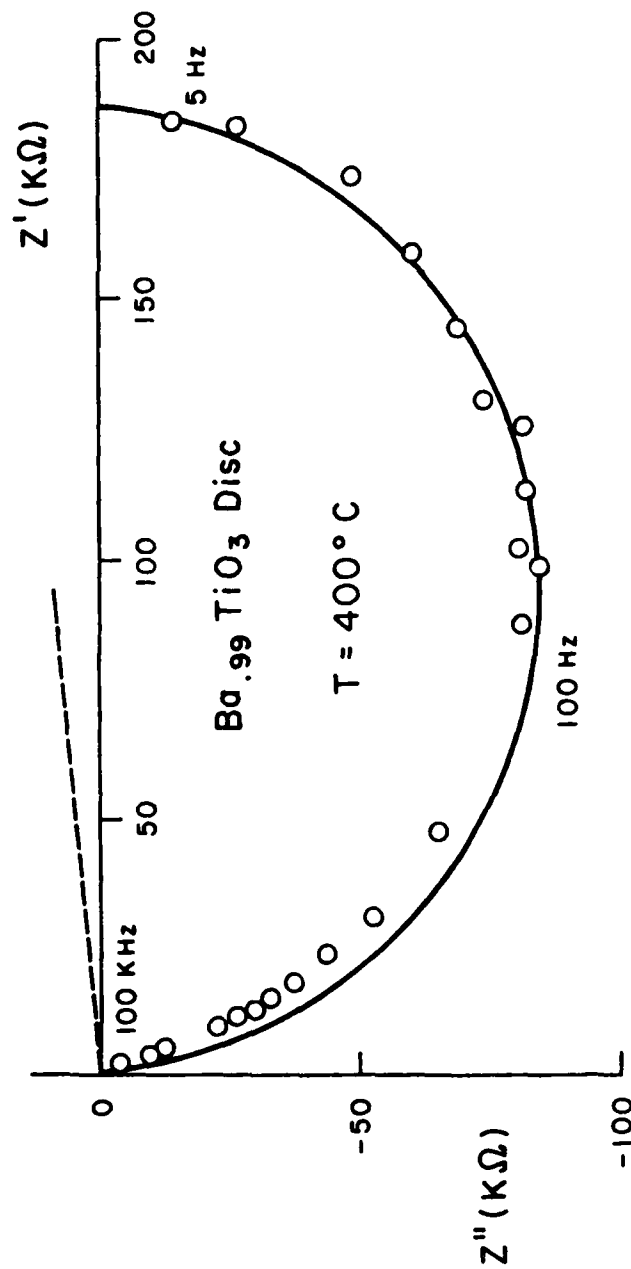


Figure 20. Impedance plot for Ba_{0.99}TiO₃ ceramic disc.

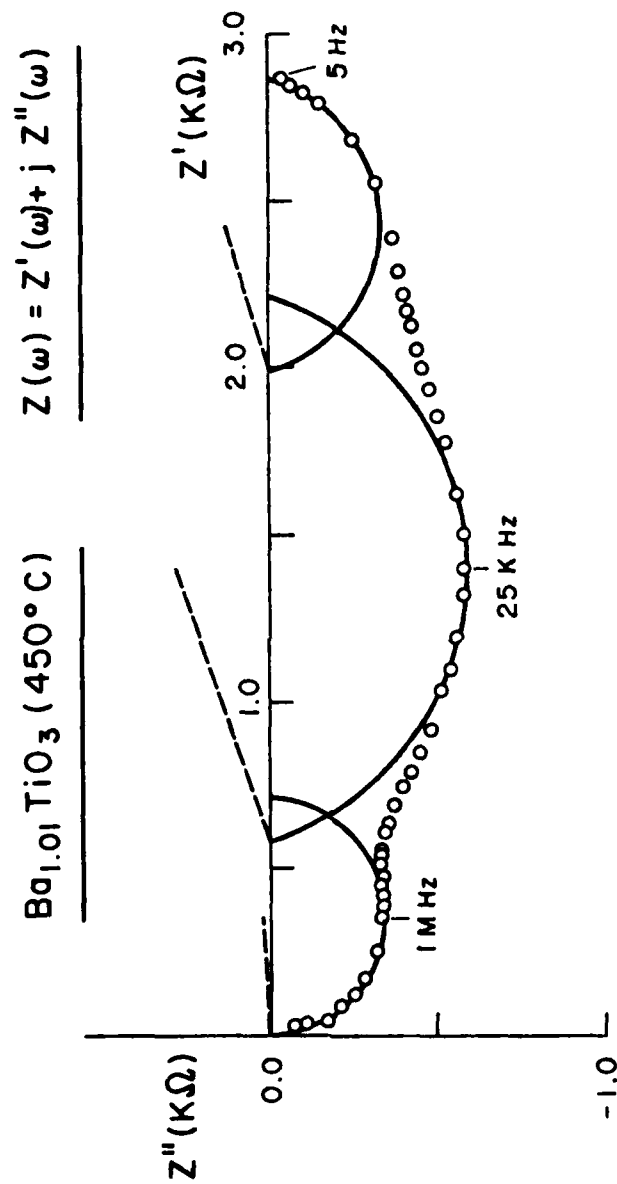


Figure 21. Impedance plot for Ba_{1.01}TiO₃ ceramic disc.

4. ELECTRODE - CERAMIC INTERFACE; DIELECTRIC THICKNESS

It is known that the nature of the electrode can have an important influence on the final properties of high-K ceramic used for MLC capacitors⁽²⁷⁾, and for thickness film capacitors⁽²⁸⁾. The role of the electrode in leakage current and degradation is not as clear.

Over this reporting period we have completed measurements on a set of non-internally electroded MCL X7R chips provided by Corning Electronics. (Some of the early measurements were discussed in the 1985 Annual Report.) Chip thicknesses varied from 2.2mm down to 0.22mm, and had a guard ring contact with Au Pt electrodes.

I-V measurements were made from 10V to 1000V at temperatures from 200°C to 350°C, in argon and air ambients. Both bulk and surface currents were measured. Major points related to the I-V curves are^(2,29). (see Figure 22):

1. There are two distinct regions of different voltage behavior: an ohmic region below transition voltage V_T (V_T depends on thickness); and a super-ohmic region above V_T .
2. The upper region depends on ambient; currents increase roughly as $V^{1.9-2.1}$ in argon, and as $V^{1.3-1.7}$ in air. The ohmic region is independent of ambient.

The upper voltage region is attributed to space charge limited currents (SCLC), whose injection efficiency depends on an ambient-dependent electrode-ceramic interface. The ohmic region is ambient independent, therefore only a very thin layer is changed by the ambient. This is consistent with the fact that changing the ambient had no effect on surface current.

Measurements made on chips polished to different thicknesses are shown in Figure 23 (in air at 250°C). A super-ohmic region is seen in all cases at higher voltages, and the ohmic to SCLC transition voltage V_T decreases linearly with sample thickness d (Figure 24).

A linear dependence of V_T on thickness is not expected for planar SCLC ($V_T \propto d^2$) is expected. For a spherical cathode emitting to a planar anode, V_T should ideally be independent of thickness⁽³⁰⁾. It is interesting that our result ($V_T \propto d$) is in between these two cases.

A linear dependence of V_T on d requires that both the ohmic and SCLC regions be power functions of electric field V/d , i.e. V/d for the ohmic case and $(V/d)^n$ with $1.3 < n < 2.1$ for SCLC.

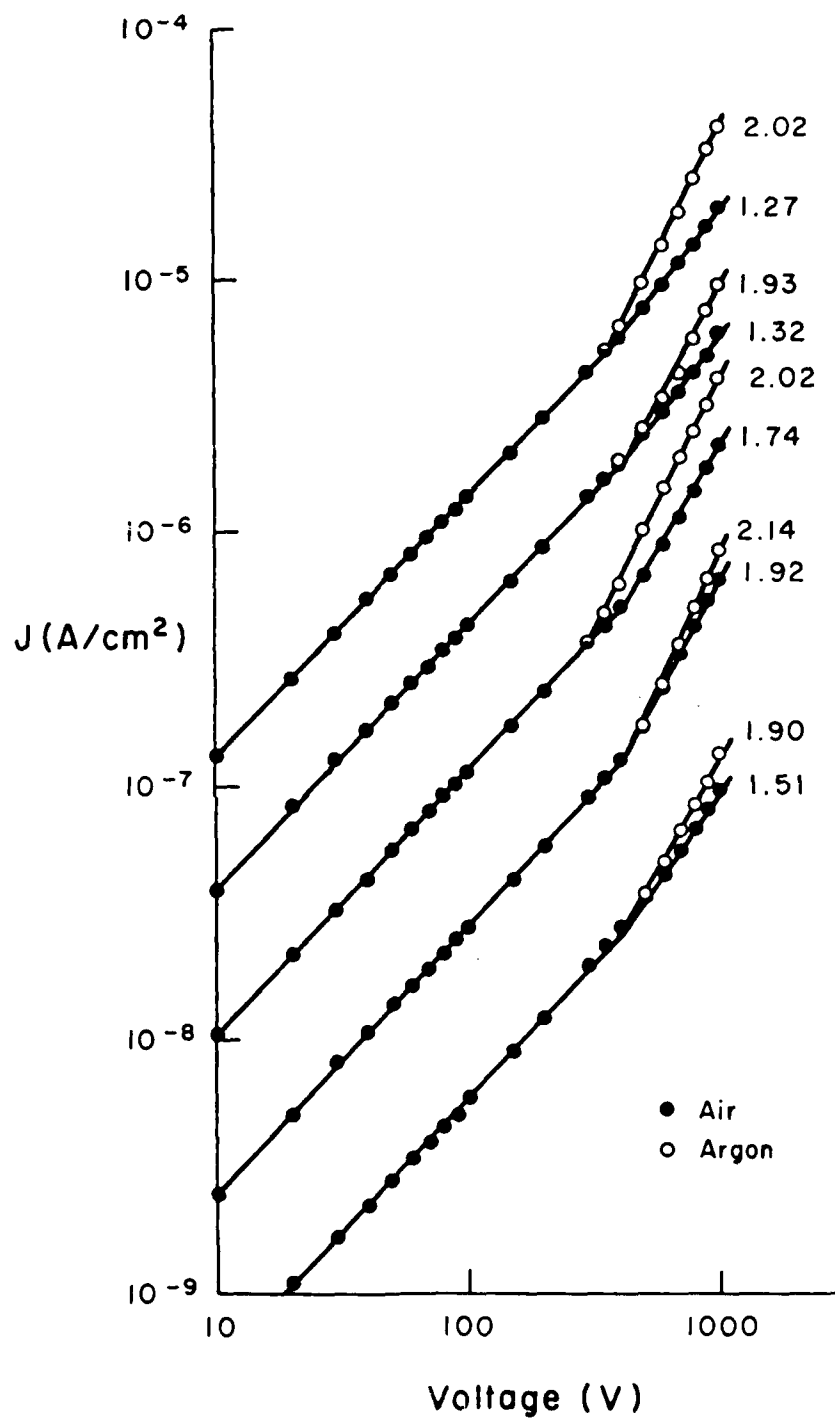


Figure 22. Current versus voltage for X7R plate at different temperatures (200-350°C), in air and argon ambients.

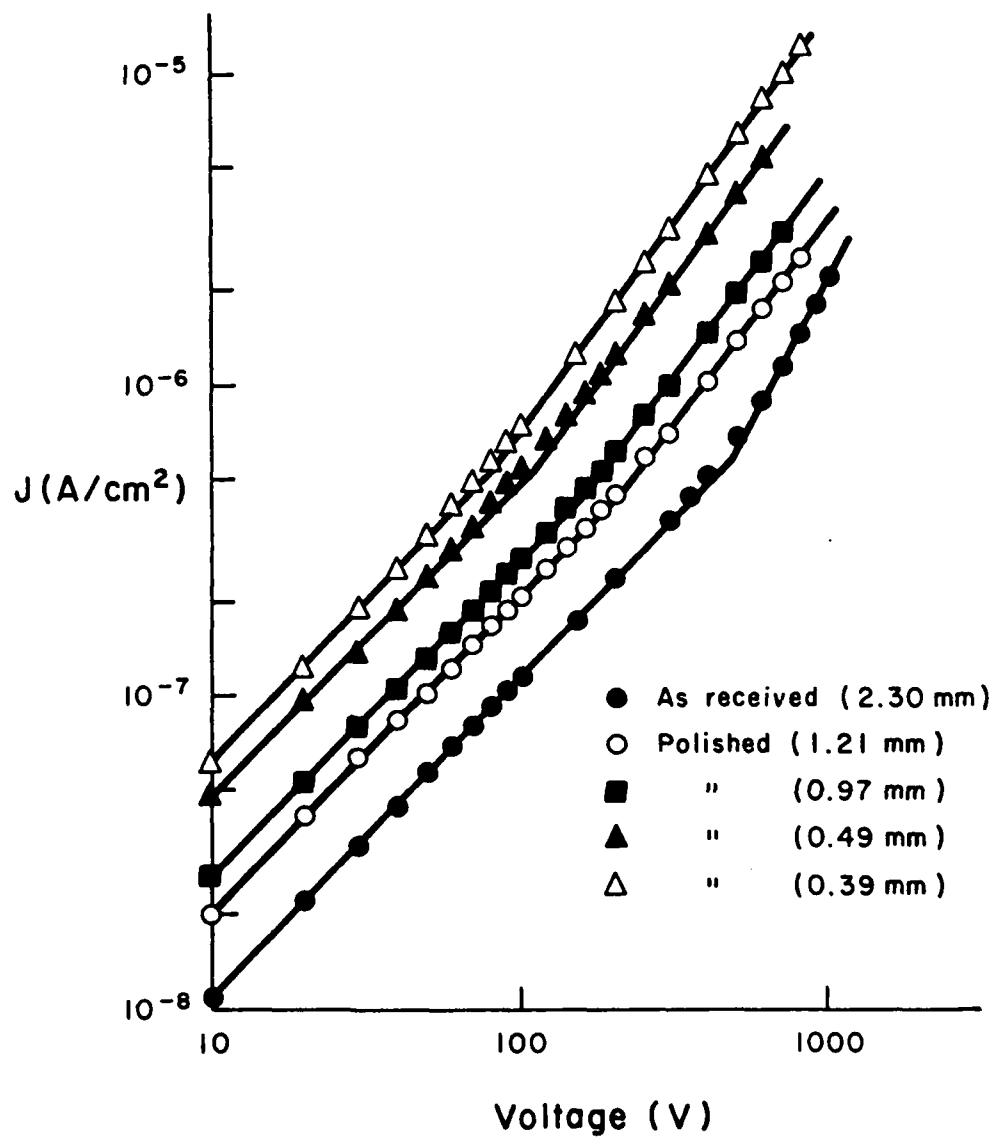


Figure 23. Current versus voltage for X7R plates of different thickness.

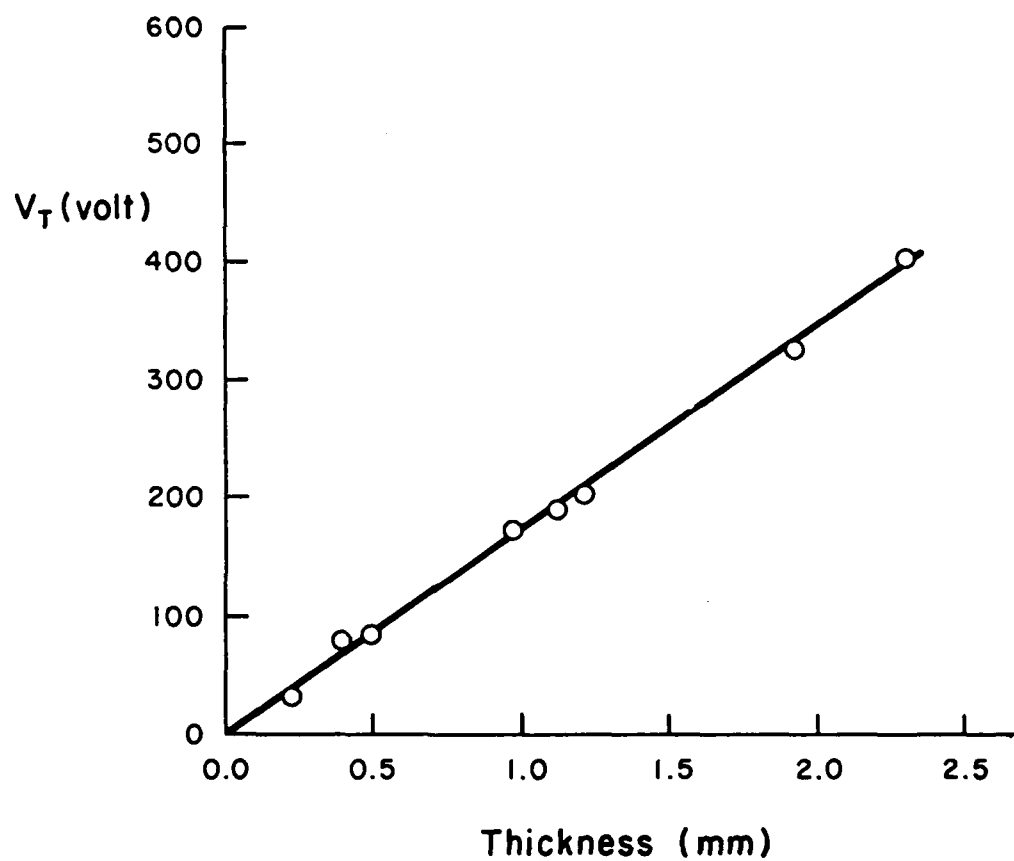


Figure 24. Ohmic to SCLC transition voltage (V_T) versus sample thickness.

Electrical parameters for these chips are summarized in Table 1. It is seen that resistivity (DC, 250°C) and dielectric constant (1KHz, room temp.) are essentially independent of thickness. This indicates that the parameters are bulk quantities and that contact effects are not important for these parameters.

Table 1
Electrical Parameters of X7R Chips

<u>d(mm)</u>	<u>SCLC Slope</u>	<u>Ohmic Resistivity</u>	<u>Dielectric Constant</u>
2.30	1.3-1.8	$4.1 \times 10^{-9} \Omega \text{cm}$	2830
1.92	1.4	3.5	2878
1.21	1.3	4.1	2300
1.12	1.3	4.1	2430
0.97	1.3	3.9	2320
0.49	1.3	4.3	-
0.39	1.4	4.2	-
0.22	1.2	5.3	2880

For a given chip, V_T is independent of temperature, as seen in Figure 25, for chips of 1.21 and 2.30mm thickness. This means that the voltage prefactors for the two current regimes have equal temperature dependences. The ohmic prefactor is $nq\mu/d$ where symbols have their usual meanings. Most SCLC models have current proportional to μ (mobility). Thus, a temperature independent V_T is consistent with the fact that carrier concentration n is nearly constant⁽³⁾, and both ohmic and SCLC currents are proportional to μ .

For comparison, I-V characteristics of a 100nF X7R capacitor, made from material similar to that of the chips, are shown in Figure 26. Since from the data of Figure 24, transition voltage varies with thickness as $V_T = 172d$ (d in mm), the MLC capacitor with $d = 1.5\text{mil}$ should be ohmic below about 6 volts. Such a transition in the 1-10 volt range has been reported⁽¹⁸⁾.

5. INSTRUMENTATION

Over this reporting period, the leakage current setup was automated. Up to 10 devices can be monitored under temperature and voltage stress, with leakage currents scanned by a Keithley 705 scanner and measured by a Keithley 617 electrometer. Control, data storage and manipulation are provided by an IBM PC-XT, with hardcopy provided by an Okidata printer. Software was developed at Virginia Tech. It is planned to add a plotter in the near future.

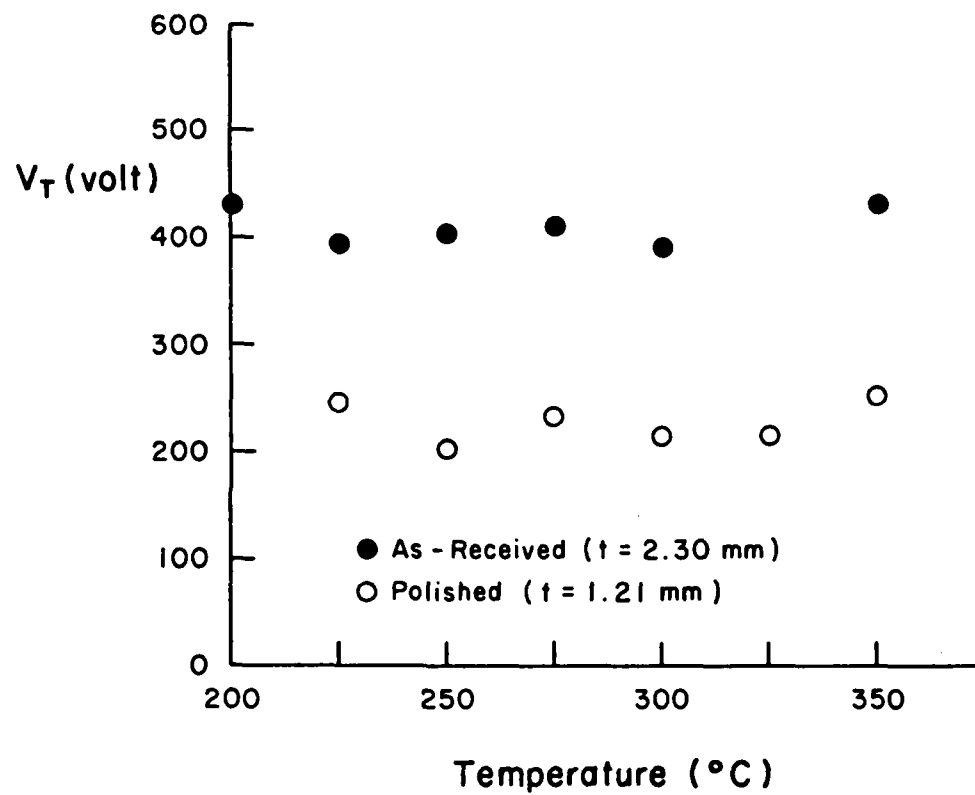


Figure 25. Transition voltage (V_T) versus temperature for two X7R chips.

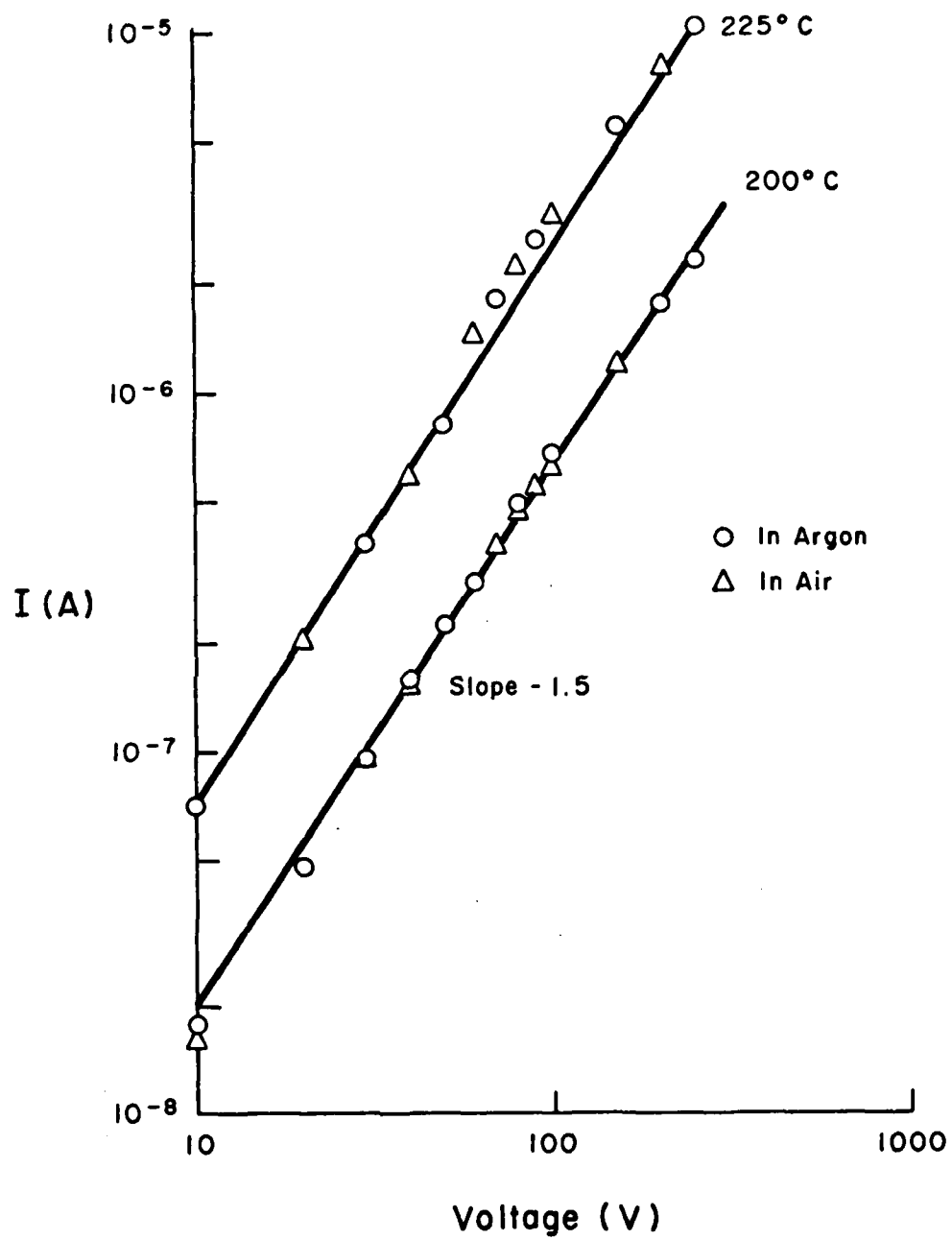


Figure 26. Current versus voltage for X7R MLC capacitor chip, in air and argon ambients.

6. FUTURE WORK

Our most immediate tasks are the following:

To separate the grain boundary contribution (if any) to insulation resistance from the total for NPO, X7R and Z5U ceramic and capacitors using complex impedance measurements combined with voltage and temperature bias;

To continue Galvanic measurements on additional BaTiO₃ based samples at higher temperatures (> 700°C) to see if oxygen conduction becomes evident;

To continue other measurements (I vs V, T, t, etc.) as necessary, and modelling of leakage current and degradation mechanisms.

ACKNOWLEDGEMENTS

In addition to the Office of Naval Research, who sponsored this work, we would like to acknowledge Corning Electronics (Neal Kenny) and MRL/Penn State (Dean Anderson) for providing samples.

REFERENCES

1. Willaim J. Minford, "Accelerated Life Testing and Reliability of High K Multilayer Ceramic Capacitors," IEEE Transactions, CHMT-S, 297 (1982).
2. "Intrinsic Mechanisms of Multilayer Ceramic Capacitor Failure", Annual Reports (April 1984, April 1985) ONR Contract No. N00014-83-K-0168 (L. C. Burton).
3. H. Y. Lee, K. C. Lee, J. N. Schunke and L. C. Burton, "Leakage Currents in Multilayer Ceramic Capacitors", IEEE Transactions CHMT-7, 443 (1984).
4. J. Stuke, "Thermoelectric Power of Amorphous Silicon and Germanium," Philosoph. Mag. B 52, 225 (1985); T. H. Geballe and G. W. Hull, Phys. Rev. 98, 940 (1955).
5. K. Kiukkola and C. Wagner, "Measurements on Galvanic Cells Involving Solid Electrolytes," J. ElectroChem. Soc., 104, 379 (1957).
6. C. Pascual, J. R. Jurado and P. Suran, "Electrical Behavior of Doped Yttria Stabilized Zirconia Ceramic Materials", J. Mater. Sci. 18, 1315 (1983).
7. S. Shirasaki et al., "Defect Structure and Oxygen Diffusion in Undoped and La-doped Polycrystalline Barium Titanate", J. Chem. Phys. 73, 4640 (1980).
8. H. V. Anderson and D. E. Day, "Reliability Studies of Ceramic Capacitors", Progress Report, ONR Contract No. N00014-82-K-0294 (July 1983).
9. S. R. Hofstein, "Space Charge Limited Tonic Currents in Silicon Dioxide Films", Appl. Phys. Lett. 10, 291 (1967); I. Bunget and M. Popescu, *Physics of Solid Dielectrics*, Elsevier (1984).
10. Yu. V. Zabara et al., "Space Charge Limited Currents in Barium Titanate Single Crystals", phys. stat. sol. (a) 38, K131 (1976); A. Branwood, et al., "Evidence of Space Charge Conduction in Barium Titanate Single Crystals", Proc. Phys. Soc. 79, 1161 (1962); L. Benguigi, "Electrical Phenomena in Barium Titanate Ceramics", J. Phys. Chem. Sol. 34, 573 (1973).

11. T. K. Gupta, W. G. Carlson, B. O. Hall, "Metastable Barrier Voltage ZnO Varistors", in *Grain Boundaries in Semiconductors* (Pike/ Seager/Leamy editors), Elsevier (1982); K. Iida et al. "Degradation Mechanism of Non-Ohmic Zinc Oxide Ceramics", *J. Appl. Phys.* 51, 2678 (1980)
12. R. M. Anderson and D. R. Kerr, "Evidence of Surface Asperity Mechanism of Conductivity in Oxide Grown on Polycrystalline Silicon", *J. Appl. Phys.* 48, 4835 (1977); S. Albin, "Localized Conduction in Dielectric Films", *Thin Solid Films* 86, 369 (1981); T. Hibma and H. R. Zeller, "Direct Measurement of Space Charge Injection from a Needle Electrode into Dielectrics, *J. Appl. Phys.* 59, 1614 (1986).
13. I. K. Yoo, L. C. Burton and F. W. Stephenson, "Instability of Insulation Resistance for Thick Film Capacitors", *ISHM Proceedings*, p. 83 (Anaheim, 1985).
14. H. Y. Lee and L. C. Burton, "Charge Carriers in MLC Capacitor Ceramic", to be presented at Electronic Components Conference, Seattle, (May, 1986).
15. G. E. Pike and C. H. Seager, "The DC Voltage Dependence of Semiconductor Grain Boundary Resistance", *J. Appl. Phys.* 50, 3414 (1979).
16. G. Blatter and G. Greuter, "Electrical Properties of Grain Boundaries in the Presence of Deep Bulk Traps", from *Polycrystalline Semiconductors*, ed. by G. Harbeke, Springer Verlag (1985).
17. B. S. Rawal and M. Kahn, "Grain Core-Grain Shell Structure in Barium Titanate Based Dielectrics", in *Advances in Ceramics*, vol. 1 (*Grain Boundary Phenomena in Electronic Ceramics*), edited by L. Levinson, Am. Ceram. Soc. (1981).
18. L. C. Burton, "Voltage Dependence of Activation Energy for Multilayer Ceramic Capacitors", *IEEE Transactions CHMT-8*, 517 (1985).
19. G. H. Jonker, "Equilibrium Barriers in PTC Thermistors", p. 155 in *Advances in Ceramics*, Vol. 1, L. Levinson ed., Amer. Ceram. Soc. (1981).
20. L. C. Burton, "Models for Electronic Conduction Across Cermaic Grain Boundaries", *Materials Research Society*, Boston (Dec 1985). To be published by MRS.
21. G. E. Pike and C. H. Seager, "The DC Voltage Dependence of Semiconductor Grain Boundary Resistance," *J. Appl. Phys.* 50, 3414 (1979); T. K. Gupta nd W. G. Carlson, "Barrier Voltage and its Effect on Stability of ZnO Varistor", *J. Appl. Phys.* 53, 7401 (1982).
22. H. D. Park and D. A. Payne, "Characterization of Internal Boundary Layer Capacitors", in *Grain Boundary Phenomena in Electronic Ceramics*, Am. Cer. Soc., 1981, p. 242.
23. J. E. Bauerle, "Study of Solid Electrolyte Polarization by a Complex Admittance Method", *J. Phys. Chem. Sol.* 30, 2657 (1969).
24. *Advances in Ceramics*, vols. 3 and 12 (Science and Technology of Zirconia), Amer. Ceram. Soc. (1981, 1984).
25. M. Kleitz and J. H. Kennedy, "Resolution of Multicomponent Impedance Diagrams", p. 185 in *Fast Ion Transport in Solids*, Vashishta, Mundy and Shenoy, eds., Elsevier (1979).
26. J. F. Baumard and P. Abelard, "Defect Structure and Transport Properties of ZrO₃ - Based Solid Electrolytes," in *Advances in Ceramics*, vol. 12, Claussen/Ruhle/Heuer eds., Amer. Ceram. Soc., 1984.
27. M. S. H. Chu and C. E. Hodgkins, "Ceramic and Metal Oxide Interaction in Multilayer Ceramic Capacitors", Am. Ceram. Soc. Electronics Div. Fall Meeting, Orlando, FL (Oct. 1985).
28. S. Stein, "Thick Film Materials", Engineering Foundation Conference, Santa Barbara, CA (Mar. 1986).
29. H. Y. Lee and L. C. Burton, "Influence of Electrode-Ceramic Interface on MLC Leakage Current," Am. Ceram. Soc. Electronics Div. Meeting, Orlando, FL (Oct. 1985). To be published in *Adv. in Ceramics*.
30. M. A. Lampert and P. Mark, *Current Injection in Solids*, Academic Press (1970).

APPENDIX

A. Participants

1. Dr. L. C. Burton, Principal Investigator, Professor of Electrical Engineering and Materials Engineering.
2. J. Neil Schunke, MS Degree in Materials Engineering, June 1985.
3. Hee-Young Lee, Ph.D. Candidate, Materials Engineering Science.
4. Susan S. Villamil, M.S. candidate in Materials Engineering.
5. Debra Dorner and Scott Ottinger, senior MatE students (senior project).

B. Reports, Papers and Publications

1. Larry C. Burton, "Voltage Dependence of Activation Energy for Multilayer Ceramic Capacitors," IEEE Transactions *CHMT-8*, 517-524 (1985). Presented previously at Electronic Components Conference, Washington, DC (May, 1985).
2. J. N. Schunke and L. C. Burton, "Grain Boundary Controlled Current in Multilayer Ceramic Capacitors," Amer. Ceram. Soc. Annual Meeting, Cincinnati (May 1985).
3. "Intrinsic Mechanisms of Multilayer Ceramic Capacitor Failure," ONR Contractors Review Meeting, Penn State (October, 1985).
4. H. Y. Lee and L. C. Burton, "Influence of Electrode - Ceramic Interface on MLC Leakage Current," Amer. Ceram. Soc. Electronics Division, Orlando, FL (October, 1985).
5. L. C. Burton, "Models for Electronic Conduction Across Ceramic Grain Boundaries," Materials Research Society, Boston, (December, 1985).
6. Larry C. Burton, "Physics of Leakage Current in Thin Insulating Ceramic Layers", Engineering Foundation Conference, "Ceramics in Electronics," Santa Barbara, CA (March, 1986).
7. L. C. Burton and H. Y. Lee, "Modelling of Leakage Current for High Resistance Ceramic," Amer. Ceram. Soc. Annual Meeting, Chicago (April, 1986).
8. H. Y. Lee and L. C. Burton, "Charge Carriers in MLC Capacitor Ceramic," accepted for presentation at 36th Electronic Components Conference, Seattle (May, 1986).
9. Hee-Young Lee, Susan S. Villamil and Larry C. Burton, "Grain Boundary Impedance in Ferroelectric Ceramic," accepted for presentation at International Ferroelectrics Meeting, Lehigh University (June, 1986)

END

10-86

DT/C